Journal of Stored Products Research 114 (2025) 102772

Contents lists available at ScienceDirect

Journal of Stored Products Research

journal homepage: www.elsevier.com/locate/jspr

Advances in stored-product pests control: evaluation of the efficacy of myrrh essential oil on two Tenebrionidae species through a metabolomic approach

Nickolas G. Kavallieratos [a,*], Maria C. Boukouvala [a], Demeter Lorentha S. Gidari [a], Constantin S. Filintas [a], Anna Skourti [a], Filippo Maggi [b], Marta Ferrati [b], Riccardo Petrelli [b], Eleonora Spinozzi [b], Cristina Teruzzi [c], Fabrizio Araniti [c]

[a] Laboratory of Agricultural Zoology and Entomology, Department of Crop Science, Agricultural University of Athens, 75 Iera Odos str., 11855, Athens, Greece
[b] Chemistry and Interdisciplinary Project (ChIP) Research Center, School of Pharmacy, University of Camerino, via Madonna delle Carceri, 62032, Camerino, Italy
[c] Department of Agricultural and Environmental Sciences—Production, Landscape, Agroenergy, University of Milan, 20133, Milan, Italy

ARTICLE INFO

Handling Editor: Dr Raul Guedes

Keywords:
Coleoptera
Stored-product pests
Commiphora myrrha
Natural product
Metabolome
Metabolomics profiling

ABSTRACT

The tenebrionids *Tenebrio molitor* L. and *Alphitobius diaperinus* (Panzer) are significant stored-product insects worldwide. The present study investigates the insecticidal activity and underlies metabolic disruptions induced by *Commiphora myrrha* (T.Nees) Engl. essential oil (EO) against both species. Adults and larvae were exposed to EO-treated wheat at 500 and 1000 ppm, with mortality monitored over seven days. *Commiphora myrrha* EO demonstrated significant dose- and time-dependent toxicity, achieving up to 91.1 % mortality of *A. diaperinus* larvae and 86.7 % mortality of *A. diaperinus* adults and *T. molitor* larvae at 1000 ppm, outperforming the commercial insecticide pirimiphos-methyl, except from the *T. molitor* adults. Chemical characterization via GC-MS and HPLC-DAD identified furanosesquiterpenes—especially furanoeudesma-1,3-diene, curzerene, and lindestrene—as dominant constituents. EO exposure led to pronounced metabolic perturbations, particularly in larvae, affecting pathways related to sugar metabolism, neurotransmission, oxidative stress, and energy homeostasis. Debiased sparse partial correlation (DSPC) network analyses revealed fragmented and modular metabolic reorganization under EO treatment, contrasting with the more integrated disruptions induced by pirimiphos-methyl. These patterns suggest distinct biochemical responses to botanical versus synthetic insecticides. Overall, *C. myrrha* EO emerged as a potent candidate biopesticide with species- and stage-specific efficacy, supported by clear metabolomic signatures. These findings advance the understanding of plant-based pest control and highlight metabolomics as a powerful tool for unraveling insecticide mechanisms.

1. Introduction

Commiphora Jacq. species play an essential role in their native landscapes, as they provide habitat and food resources for various organisms, including pollinators, herbivores, and local livestock populations (Soromessa, 2013; Gostel et al., 2016). Moreover, they are linked to income-generating activities of the human population of these areas (Mekonnen et al., 2013). *Commiphora myrrha* (T.Nees) Engl. (Burseraceae) is a keystone plant species with broad ecological, economic, and cultural importance. This small to medium-sized thorny shrub thrives in harsh environments characterized by minimal rainfall and poor soil fertility (Suleiman, 2015). It is a drought-resistant plant, originating from arid regions of northeastern Africa, like the Horn of Africa, as well as the Arabian Peninsula (Shen et al., 2012). It has been valued for the excretion of a unique oleo-gum resin, called myrrh, which has been used traditionally in medicine, religious ceremonies, and as a valuable trade commodity (Hassan et al., 2019). In recent years, *C. myrrha* has attracted the attention of researchers due to its distinctive chemical composition, including three distinctive fractions, namely essential oil (EO) (oleo), polysaccharides (gum), and triterpenoids (resin). The EO of *C. myrrha* is a complex mixture of volatile compounds, among which the fraction of furanosesquiterpenes is predominant, accounting for more than 80 % of the total EO composition (Spinozzi et al., 2025). The main constituents of this group are furanoeudesma-1,

* Corresponding author.
E-mail address: nick_kaval@aua.gr (N.G. Kavallieratos).

https://doi.org/10.1016/j.jspr.2025.102772
Received 6 June 2025; Received in revised form 1 August 2025; Accepted 2 August 2025
Available online 22 August 2025

3-diene, curzerene, isofuranodiene, and lindestrene (Gadir and Ahmed, 2014). Notably, curzerene seems to be an artifact product coming from the thermal degradation, known as Cope rearrangement, of isofuranodiene, occurring during distillation of the oleo-gum resin (Spinozzi et al., 2025). These compounds have antimicrobial, mosquitocidal, cytotoxic, analgesic, anti-inflammatory, and antioxidant effects (Tipton et al., 2003; Su et al., 2011; Gadir and Ahmed, 2014; Spinozzi et al., 2025), making myrrh a valuable resource in the pharmaceutical, food, and cosmetic industries (Latha et al., 2021). Notably, the potential application of myrrh in pest management has been recently proposed (Alanazi et al., 2024).

In detail, recent research has found that extracts and EO from *C. myrrha* possess strong insecticidal properties. For instance, myrrh EO and its main furanosesquiterpenes showed efficacy against larvae of several mosquito species including those belonging to the genera *Anopheles* and *Aedes* (Spinozzi et al., 2025). Similarly, Alanazi et al. (2024) reported that the resin of *C. myrrha* induced high larval and pupal mortality to *Aedes aegypti* (L.) (Diptera: Culicidae). Additionally, the gum resin powder and methanol extract of *C. myrrha* have shown effectiveness against stored-product pests such as *Trogoderma granarium* Everts (Coleoptera: Dermestidae), through fumigant and repellent assays (Al-Fuhaid, 2017).

The tenebrionids *Tenebrio molitor* L. and *Alphitobius diaperinus* (Panzer) negatively impact 51 and 89 types of stored products, respectively (Hagstrum et al., 2013). Both species secrete benzoquinones by the abdominal glands, causing an unpleasant odor to the infested products (Rees, 2004). *Alphitobius diaperinus* is a noxious species of poultry industry, transmitting dangerous pathogenic microorganisms, like bacteria and viruses (Eidson et al., 1966; Goodwin and Waltman, 1996; Bertola and Mutinelli, 2021). In poultry houses, it causes different types of damages, including the consumption of the chickens' spilled feed (Sammarco et al., 2023).

A widespread effective, potent, and systematic analytical technique for analyzing metabolite changes is metabolomics (Feng et al., 2022; Utpott et al., 2022). This technique has been used to assess the metabolomic profile of the larvae of *T. molitor* when cultured on different rearing mediums (Ferri et al., 2024). Except for the effects of the commodities, metabolomics can be used to detect the influence of other parameters, like the environmental conditions. Engell Dahl and Renault (2022) tested the effect of the exposure to dry conditions in the activity, water content, metabolic profiles, longevity, and fecundity of *A. diaperinus*.

Both *A. diaperinus* and *T. molitor* proved to be resistant to synthetic insecticides (Mukerjea, 1953; Renault and Colinet, 2021; Gouesbet et al., 2025). In this regard, the use of botanical-based insecticides is less likely to lead to resistance (Singh et al., 2022) and the effects of EOs on these two pest species need an in-depth investigation. Thus, this research aims to explore the insecticidal activity of myrrh EO against *A. diaperinus* and *T. molitor* adults and larvae. In addition, a metabolomic assessment on treated insects has been carried out. The chemical composition of myrrh EO was determined through GC-MS and HPLC-DAD analyses. The insect species selected for the mortality bioassays are understudied regarding their response to myrrh EO, while also for their metabolomic analysis under insecticidal pressure. Since the response of the insect species to myrrh EO has never been investigated before, this study could also add significant information on its mode of action.

2. Materials and methods

2.1. Essential oil (EO) chemical characterization

The chemical composition of myrrh EO (purchased from El Taller De Aiquimia, S.L. Can Duran, Girona, Spain) was determined by following the same methodologies reported by Spinozzi et al. (2025). Specifically, the semi-quantification of the EO constituents was achieved through gas chromatography-mass spectrometry (GC-MS) analysis. The employed instrument was an Agilent 8890 gas chromatograph coupled to a 5977B single quadrupole mass spectrometer (Santa Clara, California, USA) and an autosampler PAL RTC120 (CTC Analytics AG, Zwingen, Switzerland). Molecules were ionized through an electron ionization source (EI) and carried along the column with helium flowing at 1 mL/min. The temperature of the injector was set at 280°C, while those of the transfer line, the ionization source and the mass analyzer at 280, 230, and 150°C, respectively. The column used for the separation of molecules was a HP-5MS capillary column (30 m × 250 μm × 0.25 μm). The oven temperature was programmed as follows: it was maintained at 60°C for 5 min, and then raised up to 220°C at 4°C/min. Subsequently, it was increased to 280°C at 11°C/min and held for 15 min, and finally increased to 300°C at 15°C/min and held for 0.5 min. The total run time resulted of 67 min. Data acquisition was performed in SCAN mode using a *m/z* range of 29–400. The EO was diluted in *n*-hexane at a 1:100 ratio and the solution (1 μL) was injected in split mode (1:200). Chromatograms were elaborated through the MSD ChemStation software (Agilent, Version G1701DA D.01.00) and the data analyzed using the NIST Mass Spectral Search Program for the NIST/EPA/NIH EI and NIST Tandem Mass Spectral Library v. 2.3. To identify the components of the EO, the mass spectra (MS) and the linear retention indices (RIs) found for each peak were compared with those reported in the literature (Adams, 2007; Mondello, 2015; NIST23, 2023). The RIs were determined injecting a mix of *n*-alkanes (C_7-C_{40}, Merck, Milan, Italy) and turning their retention time with the Van den Dool and Krat (1963) formula. The EO was analyzed twice, and the relative percentage of each compound was expressed as average areas (%) ± standard deviation (SD).

The quantification of isofuranodiene, curzerene, and furanoeudesma-1,3-diene was carried out through an Agilent Technologies high performance-liquid chromatograph (HPLC) HP-1100 series (Palo Alto, CA, USA), composed of an autosampler, a binary solvent pump, and a diode array detector (DAD). The molecules were separated through a Kinetex© PFP 100A column (100 × 4.6 mm internal diameter, 2.6 μm) purchased from Phenomenex (Torrance, CA). The analytical conditions, the construction of the calibration curves, and the method validation followed those previously reported by Spinozzi et al. (2025).

2.2. Insect species

Insect colonies are kept in complete dark conditions at the Agricultural University of Athens (Laboratory of Agricultural Zoology and Entomology). *Alphitobius diaperinus* was reared on the mix of wheat bran and yeast (3:1 ratio), with apple cuttings to increase moisture (Kavallieratos et al., 2024a), while *T. molitor* on oat bran and potato slices for additional moisture (Boukouvala et al., 2021). The standard temperature for all colonies was set at 30°C with 65 % relative humidity (RH) (Kavallieratos et al., 2024b). There was no sex determination for the selected individuals. The selected adults of *T. molitor* and *A. diaperinus* were under 14 days old and less than one week old, respectively (Kavallieratos et al., 2024a). The larvae of the tenebrionids were collected based on body length for the trials. Specifically, *T. molitor* and *A. diaperinus* larvae were measured to be 1–1.4 and 0.7 cm in length respectively (Kavallieratos et al., 2024a).

2.3. Grain

For the mortality assays, clean and pesticide-free *Triticum durum* Desf., var. Claudio (hard wheat) was used as substrate. Before testing, wheat moisture content was determined at 13.2 % using the C-Pro grain moisture meter (AgroLog, Søndersø, Denmark) to ensure consistency (Kavallieratos et al., 2024a).

2.4. Mortality bioassays

Following an initial evaluation of 500 and 1000 ppm concentrations (500 and 1000 μL EO/kg wheat) from preliminary trials, the bioassays

were conducted. To prepare the EO solutions, 150 and 250 μL of EO were first dissolved in pure ethanol at a 1:1 ratio (v/v) for concentrations of 500 and 1000 ppm, respectively. Tween 80 was then added to the mixtures in a 0.3 % (v/v) aqueous solution to raise the total volume to 750 μL (Kavallieratos et al., 2024a). Using the GHPM-Mobius airbrush (Gaahleri, New Jersey, USA), 0.25 kg of wheat were sprayed on separate trays to apply EO solutions; each tray represented a treatment replicate. Additional lots were treated with different solutions consisting of water, pure ethanol in water and Tween 80 (carrier control), and pure ethanol serving as negative controls or Actellic EC (positive control), which included 50 % of pirimiphos-methyl (active ingredient) at 5 ppm = 5 μL/kg wheat concentration (as suggested on the pesticide label). Separate airbrushes were used to apply each of these solutions. A 10-min manual agitation was carefully carried out after the treated wheat amounts were moved into 1-liter glass jars. The procedure was carried out to ensure that the controls and EO solutions were evenly distributed on all kernels. Next, three 10-g sub-samples (3 sub-replicates) were taken from each treated 1 L-wheat vial (EO or control) with the help of a new spoon for each treatment. The electron balance Precisa XB3200D (Alpha Analytical Instruments, Greece) was utilized for the weighting of these wheat sub-samples precisely on distinct filter paper for each weighing. Then, those sub-samples were placed into smaller glass vials (125 mm height × 75 mm diameter) and their caps had openings to allow air to circulate. To maintain the insects inside, a polytetrafluoroethylene dispersion in water (60 % by weight) (Sigma-Aldrich Chemie GmbH, Germany) was applied to the internal walls close to the vial caps. Ten individuals per sub-replicate of each species, adults or larvae, were introduced into the designated vials per replicate of controls, and EO (500 and 1000 ppm treatments). Then, the vials were placed in incubators set at the aforementioned abiotic conditions (subsection Insect species). To prevent cannibalism among individuals of *A. diaperinus*, each sub-replication included ten vials containing a single arthropod (Kavallieratos et al., 2024b). The Olympus SZX9 stereomicroscope (Bacacos S.A., Greece) was used to measure mortality following exposure intervals of 8–24 h and 2–7 days. For each treatment, dead individuals were examined carefully using separate, fine brushes to make sure that any movement from the arthropods was noted. Two more replications of the entire procedure were carried out, using fresh sets of glass vials, arthropods, and wheat per replication (Kavallieratos et al., 2024a).

2.5. Metabolomic analysis bioassays

Individuals of each species/life stage, ≈0.3 g totally, were introduced into the designated vials per replicate of control (water-negative control), 5 ppm pirimiphos-methyl (positive control), and 1000 ppm of EO. Then, the vials were placed into incubators set at the aforementioned abiotic conditions (subsection Insect species). After 24 h post exposure, the individuals (per species/life stage per treatment per replicate) were collected from the treated wheat, placed into corresponding labeled 23 ml-plastic tubes and were immersed in liquid nitrogen. Subsequently, the tubes were placed in the freezer at a temperature of −80 °C till the metabolomic extraction and analyses. Four more replicates were carried out, using fresh sets of glass vials, arthropods, and wheat per replication.

2.6. Metabolite extraction and analysis

Metabolome extraction, derivatization and analysis were carried out following the method proposed by Spinozzi et al. (2025) with some modifications. Briefly, 100 mg of larvae and adults were pulverized in liquid nitrogen and spiked with ribitol (0.2 mg/mL) to serve as an internal standard. The resulting derivatized samples were analyzed using a gas chromatograph (8890 GC System, Agilent, Santa Clara, California, USA) coupled to a single quadrupole mass spectrometer (5977C GC/MSD, Agilent, Santa Clara, California, USA) via a CTC PAL autosampler (CTC Analytics AG, Industriestrasse 20, CH-4222 Zwingen, Switzerland). The GC setup featured a 5MS column (30 m × 0.25 mm × 0.25 μm) and a 10 m precolumn. Instrumental parameters—including temperature settings, analytical conditions, and the MS-DIAL processing for baseline filtering, alignment, deconvolution, peak extraction, and annotation—were set according to the guidelines provided by Misra (2019). Quality control and monitoring of instrument performance and RI variations were maintained by routinely injecting blank solvents, quality controls (QC), and even-numbered *n*-alkane standards (C_{10}–C_{40}). Peak annotations were determined based on RIs and spectral similarity using an in-house EI spectral library, with assignments classified as level 2 and/or level 3 as per the criteria outlined by Sumner et al. (2007).

2.7. Data analysis

No adjustments were necessary for the negative control mortality, which remained below 5 % for all tested individuals. Prior to analysis, the dataset was log (x + 1) converted to standardize variance (Zar, 2014; Scheff and Arthur, 2018). Data for each species or life stage was examined separately via the model of repeated measures (Sall et al., 2001). Analyses included related interactions of the main effects. The main effects, response variable, and repeated factors were the treatment/concentrations, mortality, and exposure, respectively. For all analyses, JMP 16.2 (SAS Institute Inc, 2021) was utilized. At 0.05 level, the Tukey test (HSD) was used to separate the means (Sokal and Rohlf, 1995). The two-tailed *t*-test at n - 2 df and 0.05 probability (Snedecor and Cochran, 1989) was used to compare the two concentrations of each treatment per tested species or life stage.

A completely randomized design with five replicates was used for the metabolomic studies. Initially, the intensities obtained from MS-DIAL were normalized using the internal standard ribitol, then Log10 transformed, and finally Pareto scaled via metaboanalyst 6.0. Following normalization, unsupervised Principal Component Analysis (PCA) and supervised Partial Least-Squares Discriminant Analysis (PLS-DA) were conducted to identify and visualize metabolic variations among the experimental groups. In the resulting score plots, the Hotelling's T^2 region—illustrated as an ellipse—marks the 95 % confidence interval of the model's variance. Variables with a Variable Importance in Projection (VIP) score exceeding 1 were considered significant for distinguishing between groups. To minimize overfitting, a permutation test (n = 20) was employed, validating the model if the empirical *p*-values for Q^2 and R^2Y were ≤0.05 and if these values approached "1". Furthermore, pairwise partial correlations among metabolites were computed using Debiased Sparse Partial Correlation (DSPC) with a degree cutoff of 2, thereby assessing the direct relationships between two metabolites while controlling for others (Basu et al., 2017). Subsequent data were analyzed through univariate one-way ANOVA ($P \leq 0.05$), with *P*-values adjusted using the False Discovery Rate (FDR ≤0.05), highlighting significant features altered by the treatments. Finally, a pathway analyses was executed to identify the pathways highly impacted by the treatments.

3. Results

3.1. Essential oil (EO) chemical composition

The chemical composition of myrrh EO was determined by GC-MS analysis, which led to the identification of the 97.8 ± 0.0 % of the volatile compounds. The most abundant class was that of furanosesquiterpenes (86.1 %), followed by sesquiterpene hydrocarbons (9.2 %) and oxygenated sesquiterpenes (0.9 %). Furanoeudesma-1,3-diene resulted to be the most abundant compound accounting for the 40.2 ± 0.0 % of the total composition. Among furanosesquiterpenes, curzerene (26.1 ± 0.1 %) and lindestrene (12.9 ± 0.0 %) were also found in high percentages, while (*R*)(5*E*,9*E*)-8-methoxy-3,6,10-trimethyl-4,7,8,11-tetrahydrocyclodeca[b]furan (4.6 ± 0.0 %), isofuranodiene (1.8 ± 0.1 %), atractylon (0.4 ± 0.0 %), and

furanoeudesma-1,4-diene (0.3 ± 0.0 %) were detected in minor percentages. The main representative of the sesquiterpene hydrocarbons was *β*-elemene (3.4 ± 0.0 %), followed by germacrene B (1.8 ± 0.0 %). Concerning oxygenated sesquiterpenes, elemol acetate (1.4 ± 0.0 %) was the predominant one (Table 1).

The HPLC-DAD analysis was performed to avoid the thermal degradation of furanosesquiterpees. The results (Table 2) confirmed the predominance of furanoeudesma-1,3-diene (67.3 ± 0.6 g/100 g EO) and the higher content in curzerene (18.4 ± 0.2 g/100 g EO) if compared to isofuranodiene (6.2 ± 0.0 g/100 g EO).

3.2. Main effects and interactions on A. diaperinus and T. molitor mortality

The analysis of the results indicates that exposure was significant across all species. Concerning effects between exposures, concentration was significant in all cases, except for *T. molitor* adults. Additionally, formulation was significant across all tested individuals, apart from the larval stage of *A. diaperinus*. The respective interaction of these main effects proved to be significant for both stages of *A. diaperinus*. Within exposure, all interactions were significant for adults and larvae of *A. diaperinus* and larvae of *T. molitor*. Concerning *T. molitor* adults, the only significant interaction was exposure x formulation (Table 3).

Table 2
Results of the HPLC-DAD analysis of *Commiphora myrrha* essential oil (EO).

Compound	g/100g EO[a] ± SD[b]	RSD %[c]
furanoeudesma-1,3-diene	67.3 ± 0.6	0.9
isofuranodiene	6.2 ± 0.0	0.4
curzerene	18.4 ± 0.2	0.9

[a] The value is the mean of two independent analysis.
[b] SD, standard deviation.
[c] RSD %, relative SD %.

3.3. Efficacy of C. myrrha EO against T. molitor adults and larvae

Concerning *T. molitor* adults, there was almost zero mortality recorded in any treatment during the first 16 h. By day 3, mortality surpassed 13.3 % (500 ppm of EO) and remained moderate until the end of the bioassay, reaching 38.9 %. At 1000 ppm of EO, there was a gradual elevation of mortality, although it also remained moderate at the end of the bioassays (66.7 %). Pirimiphos-methyl provided almost identical mortality rates to the 1000-ppm EO treatment, across the exposure period, reaching 67.8 % (Table 4).

Larvae of the same species exhibited a delayed initial lethal response to the EO treatments, due to the almost zero documented mortality rates of the first hours and first day. The lower concentration provided a slow

Table 1
Chemical composition of *Commiphora myrrha* essential oil (EO).

No[a]	Compound	RI[b]	RI Lit[c]	% ± SD[d]
1	*δ*-elemene	1336	1335	0.5 ± 0.0
2	*α*-copaene	1373	1374	tr[e]
3	*β*-bourbonene	1382	1387	0.2 ± 0.0
4	*β*-elemene	1390	1389	3.4 ± 0.0
5	cyperene	1396	1398	tr
6	*(E)*-caryophyllene	1416	1417	0.3 ± 0.0
7	*β*-copaene	1426	1430	tr
8	γ-elemene	1432	1434	0.5 ± 0.0
9	*α*-humulene	1451	1452	0.1 ± 0.0
10	γ-muurolene	1474	1478	0.1 ± 0.0
11	germacrene D	1479	1484	0.5 ± 0.0
12	*β*-selinene	1483	1489	0.5 ± 0.0
13	*α*-selinene	1492	1498	0.5 ± 0.0
14	curzerene	1495	1499	26.1 ± 0.1
15	*δ*-amorphene	1505	1511	tr
16	*γ*-cadinene	1512	1513	0.1 ± 0.0
17	*δ* -cadinene	1522	1522	0.2 ± 0.0
18	zonarene	1533	1528	tr
19	selina-3,7-(11)-diene	1539	1545	0.1 ± 0.0
20	*α*-calacorene	1541	1544	0.0 ± 0.0
21	germacrene B	1554	1559	1.8 ± 0.0
22	furanoeudesma-1,4-diene	1576	1587	0.3 ± 0.0
23	curzerenone	1603	1605	0.1 ± 0.0
24	furanoeudesma-1,3-diene	1624	1625	40.2 ± 0.0
25	lindestrene	1631	1632	12.9 ± 0.0
26	*epi*-*α*-cadinol	1639	1638	0.5 ± 0.0
27	atractylone	1654	1657	0.4 ± 0.0
28	elemol acetate	1676	1680	1.4 ± 0.0
29	isofuranodiene	1689	1690	1.8 ± 0.1
30	germacrone	1693	1693	0.4 ± 0.0
31	(*R*)(5*E*,9*E*)-8-methoxy-3,6,10-trimethyl-4,7,8,11-tetrahydrocyclodeca[b]furan	1719	1719	4.6 ± 0.0
32	*β*-eudesmol acetate	1785	1792	0.1 ± 0.0
33	*α*-eudesmol acetate	1787	1794	0.1 ± 0.0
	Total identified			97.8 ± 0.0
	Sesquiterpene hydrocarbons			9.2
	Furanosesquiterpenes			86.1
	Oxygenated sesquiterpenes			0.9
	Esters			1.5

[a] Compounds are reported according to their elution order from a HP-5MS capillary column.
[b] Linear retention index experimentally calculated with the Van den Dool and Kratz formula considering the retention time of a homologue mixture of *n*-alkanes (C_7–C_{40}).
[c] Linear retention index reported in the literature.
[d] Average % referring to two independent analysis ± standard deviation.
[e] Traces.

Table 3
MANOVA parameters showing the main effects and their interactions leading to the observed mortalities of *Tenebrio molitor* and *Alphitobius diaperinus* adults and larvae, between and within exposures (error df = 32 for all species).

		Between exposures				Within exposures			
		Intercept	Concentration	Formulation	Concentration x formulation	Exposure	Exposure x concentration	Exposure x formulation	Exposure x concentration x formulation
df		1	1	1	1	9	9	9	9
T. molitor adults	*F*	1665.7	2.9	4.6	2.3	1386.8	1.8	2.5	2.0
	P	<0.01	0.10	0.04	0.14	<0.01	0.13	0.03	0.09
T. molitor larvae	*F*	868.3	6.5	35.3	0.2	1272.3	2.3	15.1	2.3
	P	<0.01	0.02	<0.01	0.63	<0.01	0.05	<0.01	0.05
A. diaperinus adults	*F*	3127.9	11.3	403.0	7.4	7673.5	7.3	375.3	9.8
	P	<0.01	0.01	<0.01	0.01	<0.01	<0.01	<0.01	<0.01
A. diaperinus larvae	*F*	1236.8	14.8	1.4	7.0	191.0	6.1	5.5	2.8
	P	<0.01	0.01	0.25	0.01	<0.01	0.01	0.01	0.02

Table 4
Mean (%) mortality ± standard errors (SE) of *Tenebrio molitor* adults after 4–16 h, and 1–7 days in wheat treated with *Commiphora myrrha* essential oil (EO) and with pirimiphos-methyl (positive control). For each concentration, within each row, asterisks indicate significant differences (df = 16; two-tailed *t*-test at *P* = 0.05). For each concentration, within each column, means followed by the same uppercase letter are not significantly different (df = 9, 89; Tukey HSD test at *P* = 0.05). No significant differences were recorded where no asterisks exist. No statistical analysis was performed where dashes exist.

	C. myrrha EO	Pirimiphos-methyl			*C. myrrha* EO	Pirimiphos-methyl		
Dose	500 ppm	Label dose (5 ppm)			1000 ppm	Label dose (5 ppm)		
Exposure			*t*	*P*			*t*	*P*
4 h	0.0 ± 0.0 E	0.0 ± 0.0 E	–	–	0.0 ± 0.0 D	0.0 ± 0.0 E	–	–
8 h	0.0 ± 0.0 E	0.0 ± 0.0 E	–	–	0.0 ± 0.0 D	0.0 ± 0.0 E	1.0	0.35
16 h	0.0 ± 0.0 E	1.1 ± 1.1 E	1	0.33	0.0 ± 0.0 D	1.1 ± 1.1 E	1.0	0.33
1 d	3.3 ± 1.7 D	8.9 ± 2.0 D*	2.1	0.05	11.1 ± 4.2 C	8.9 ± 1.1 D	0.8	0.42
2 d	10.0 ± 1.7 C	13.3 ± 2.4 CD	0.5	0.62	20.0 ± 5.3 BC	11.1 ± 2.0 CD	−0.7	0.46
3 d	13.3 ± 1.7 BC	22.2 ± 3.2 BC*	2.4	0.03	26.7 ± 3.7 AB	22.2 ± 4.0 BC	−0.9	0.36
4 d	22.2 ± 2.8 AB	31.1 ± 2.6 AB*	2.4	0.03	31.1 ± 4.5 AB	33.3 ± 2.9 AB	0.7	0.48
5 d	24.4 ± 2.4 AB	41.1 ± 4.2 AB*	3.5	0.01	37.8 ± 4.7 AB	42.2 ± 2.8 AB	1.1	0.31
6 d	32.2 ± 2.8 A	52.2 ± 3.2 A*	4.7	0.01	47.8 ± 5.7 A	54.4 ± 3.8 A	1.2	0.26
7 d	38.9 ± 3.9 A	65.6 ± 3.8 A*	4.9	0.01	66.7 ± 6.7 A	67.8 ± 2.2 A	0.5	0.63
F	82.2	76.6			54.9	100.5		
P	<0.01	<0.01			<0.01	<0.01		

Table 5
Mean (%) mortality ± standard errors (SE) of *Tenebrio molitor* larvae after 4–16 h, and 1–7 days in wheat treated with *Commiphora myrrha* essential oil (EO) and with pirimiphos-methyl (positive control). For each concentration, within each row, asterisks indicate significant differences (df = 16; two-tailed *t*-test at *P* = 0.05). For each concentration, within each column, means followed by the same uppercase letter are not significantly different (df = 9, 89; Tukey HSD test at *P* = 0.05). No significant differences were recorded where no asterisks exist. No statistical analysis was performed where dashes exist.

	C. myrrha EO	Pirimiphos-methyl			*C. myrrha* EO	Pirimiphos-methyl		
Dose	500 ppm	Label dose (5 ppm)			1000 ppm	Label dose (5 ppm)		
Exposure			*t*	*P*			*t*	*P*
4 h	0.0 ± 0.0 D	0.0 ± 0.0 E	–	–	0.0 ± 0.0 E	0.0 ± 0.0 C	–	–
8 h	0.0 ± 0.0 D	0.0 ± 0.0 E	–	–	0.0 ± 0.0 E	0.0 ± 0.0 C	–	–
16 h	0.0 ± 0.0 D	0.0 ± 0.0 E	–	–	0.0 ± 0.0 E	0.0 ± 0.0 C	–	–
1 d	0.0 ± 0.0 D	2.2 ± 1.5 DE	1.5	0.15	2.2 ± 1.5 E	1.1 ± 1.1 C	−0.6	0.55
2 d	6.7 ± 2.4 C	3.3 ± 1.7 DE	−1.0	0.33	12.2 ± 2.2 D*	3.3 ± 1.7 C	−3.1	0.01
3 d	12.2 ± 2.2 B*	4.4 ± 1.8 CDE	−2.4	0.03	21.1 ± 2.6 CD*	7.8 ± 1.5 B	−3.2	0.01
4 d	32.2 ± 2.2 A*	6.7 ± 1.7 BCD	−4.6	0.01	41.1 ± 3.1 BC*	13.3 ± 2.4 AB	−7.7	<0.01
5 d	40.0 ± 2.4 A*	14.4 ± 3.8 ABC	−3.3	0.01	52.2 ± 3.6 AB*	16.7 ± 3.3 AB	−6.6	<0.01
6 d	43.3 ± 5.3 A*	18.9 ± 3.5 AB	−2.8	0.01	61.1 ± 5.9 AB*	23.3 ± 4.7 A	−4.7	0.01
7 d	53.3 ± 2.9 A*	31.1 ± 3.1 A	−5.1	<0.01	86.7 ± 3.3 A*	32.2 ± 3.2 A	−11.7	<0.01
F	97.6	15.5			140.6	43.7		
P	<0.01	<0.01			<0.01	<0.01		

and steady increase up to 53.3 % on the last day. Additionally, the highest concentration proved to be more toxic to the larvae of *T. molitor*, with substantial rates being documented from the third day onward. By day 7, mortality peaked at 86.7 %. Positive control mortality rates did not exceed 33.0 % even at the end of the trials (Table 5).

3.4. Efficacy of C. myrrha EO against A. diaperinus adults and larvae

Concerning the adults of *A. diaperinus*, no mortality was recorded during the first 8 h of exposure. On the 16 h, both EO concentrations achieved low initial mortality rates that had a similar gradual increase of approximately 10 % per day, reaching 47.8 and 86.7 % at 500 and 1000 ppm, respectively, on day 7. Pirimiphos-methyl caused minimal mortality during the three-day period, and it peaked at 23.3 % on the last

Table 6
Mean (%) mortality ± standard errors (SE) of *Alphitobius diaperinus* adults after 4–16 h, and 1–7 days in wheat treated with *Commiphora myrrha* essential oil (EO) and with pirimiphos-methyl (positive control). For each concentration, within each row, asterisks indicate significant differences (df = 16; two-tailed *t*-test at $P = 0.05$). For each concentration, within each column, means followed by the same uppercase letter are not significantly different (df = 9, 89; Tukey HSD test at $P = 0.05$). No significant differences were recorded where no asterisks exist. No statistical analysis was performed where dashes exist.

	C. myrrha EO	Pirimiphos-methyl			*C. myrrha* EO	Pirimiphos-methyl		
Dose	500 ppm	Label dose (5 ppm)			1000 ppm	Label dose (5 ppm)		
Exposure			*t*	*P*			*t*	*P*
4 h	0.0 ± 0.0 E	0.0 ± 0.0 B	–	–	0.0 ± 0.0 E	0.0 ± 0.0 C	–	–
8 h	0.0 ± 0.0 E	0.0 ± 0.0 B	–	–	0.0 ± 0.0 E	0.0 ± 0.0 C	–	–
16 h	7.8 ± 1.5 D*	0.0 ± 0.0 B	−5.3	0.01	11.1 ± 3.5 D*	0.0 ± 0.0 C	−3.2	0.01
1 d	11.1 ± 1.1 C*	0.0 ± 0.0 B	−34.4	<0.01	24.4 ± 1.8 C*	0.0 ± 0.0 C	−47.0	<0.01
2 d	15.6 ± 1.8 C*	0.0 ± 0.0 B	−24.3	<0.01	33.3 ± 2.4 BC*	0.0 ± 0.0 C	−46.8	<0.01
3 d	20.0 ± 1.7 BC*	3.3 ± 2.4 B	−5.8	0.01	41.1 ± 1.1 ABC*	4.4 ± 1.8 B	−6.3	0.01
4 d	30.0 ± 1.7 AB*	13.3 ± 2.4 A	−6.0	<0.01	51.1 ± 1.1 ABC*	14.4 ± 1.8 A	−11.0	<0.01
5 d	33.3 ± 2.4 AB*	20.0 ± 2.9 A	−3.3	0.01	57.8 ± 2.2 AB*	18.9 ± 2.6 A	−8.0	<0.01
6 d	40.0 ± 1.7 A*	22.2 ± 2.2 A	−5.2	0.01	68.9 ± 2.6 AB*	21.1 ± 2.6 A	−8.6	<0.01
7 d	47.8 ± 3.6 A*	23.3 ± 2.4 A	−5.2	0.01	86.7 ± 2.9 A*	23.3 ± 2.4 A	−11.2	<0.01
F	122.7	97.8			96.5	89.7		
P	<0.01	<0.01			<0.01	<0.01		

Table 7
Mean (%) mortality ± standard errors (SE) of *Alphitobius diaperinus* larvae after 4–16 h, and 1–7 days in wheat treated with *Commiphora myrrha* essential oil (EO) and with pirimiphos-methyl (positive control). For each concentration, within each row, asterisks indicate significant differences (df = 16; two-tailed *t*-test at $P = 0.05$). For each concentration, within each column, means followed by the same uppercase letter are not significantly different (df = 9, 89; Tukey HSD test at $P = 0.05$). No significant differences were recorded where no asterisks exist.

	C. myrrha EO	Pirimiphos-methyl			*C. myrrha* EO	Pirimiphos-methyl		
Dose	500 ppm	Label dose (5 ppm)			1000 ppm	Label dose (5 ppm)		
Exposure			*t*	*P*			*t*	*P*
4 h	0.0 ± 0.0 C	1.1 ± 1.1 F	1.0	0.35	0.0 ± 0.0 G	1.1 ± 1.1 D	1.0	0.33
8 h	0.0 ± 0.0 C	3.3 ± 1.7 EF	2.0	0.08	0.0 ± 0.0 G	3.3 ± 1.7 CD	2.0	0.08
16 h	0.0 ± 0.0 C	4.4 ± 1.8 DEF*	2.5	0.04	8.9 ± 1.1 F	6.7 ± 2.4 BCD	−1.4	0.19
1 d	2.2 ± 1.5 C	6.7 ± 1.7 CDE	2.0	0.06	18.9 ± 1.1 E*	10.0 ± 3.3 BC	−2.5	0.03
2 d	8.9 ± 2.0 B	12.2 ± 3.2 BCD	0.3	0.74	28.9 ± 2.6 DE	17.8 ± 3.6 AB	−1.9	0.09
3 d	14.4 ± 1.8 B	17.8 ± 2.2 ABC	1.1	0.29	37.8 ± 2.2 CD*	24.4 ± 3.4 A	−3.0	0.01
4 d	31.1 ± 1.1 A*	21.1 ± 3.1 AB	−3.1	0.01	52.2 ± 2.8 BC*	28.9 ± 2.6 A	−4.6	0.01
5 d	38.9 ± 2.0 A*	28.9 ± 3.1 AB	−2.8	0.02	63.3 ± 2.4 AB*	30.0 ± 2.9 A	−5.8	0.01
6 d	46.7 ± 2.9 A*	34.4 ± 2.9 A	−2.8	0.01	75.6 ± 2.9 AB*	34.4 ± 3.6 A	−5.4	0.01
7 d	60.0 ± 1.7 A*	36.7 ± 2.4 A	−7.4	<0.01	91.1 ± 2.0 A*	37.8 ± 2.8 A	−10.2	<0.01
F	107.0	18.8			282.6	17.6		
P	<0.01	<0.01			<0.01	<0.01		

day of the trials (Table 6).

For the *A. diaperinus* larvae, mortality remained negligible across all treatments during the first 16-h exposure period. At 500 ppm of the EO, mortality rates increased significantly, although they remained moderate, reaching 60.0 % by the end of trials. At 1000 ppm EO concentration, initial mortality was documented earlier by 16 h (8.9 %), and it showed a gradual elevation up to 91.1 % on the seventh day of exposure. Pirimiphos-methyl induced minimal rates on the first h of exposure, and after a steady increase it peaked just above 36.0 % (Table 7).

3.5. Effects of C. myrrha EO on A. diaperinus and T. molitor larval metabolome

The PCA analysis reveals that the first two components explain about 75 % of the total variance, with PC1 accounting for roughly 53.3 % and PC2 for about 21.4 % (Fig. 1a). This analysis clearly distinguishes the two species: *A. diaperinus* clusters on the negative side of PC1, while *T. molitor* clusters on the positive side, indicating inherent differences between them. Within each species, the treatments further separate along PC2 (Fig. 1a). For instance, in *A. diaperinus*, the control larvae form a distinct group. At the same time, those treated with the EO and pirimiphos-methyl occupy separate positions along this axis. A similar pattern is observed in *T. molitor*, where each treatment, control, EO, and pirimiphos-methyl, leads to unique clustering. These findings suggest that both the species identity and the type of treatment significantly influence the measured variables, resulting in clearly defined groupings on the PCA plot (Fig. 1a).

In the loadings plot, several sugars (sucrose, arabinose, xylose, xylitol, and trehalose) are positioned far from the origin and thus exert a strong influence on the first two principal components, with sucrose being shifted toward the positive side of PC1. In contrast, arabinose and xylose appear more negative (Fig. 1b). Amines and neurotransmitter-related compounds (i.e., dopamine, norepinephrine, GABA, and putrescine) cluster in the upper-right quadrant, suggesting that they also drive separation along PC2 (Fig. 1b). By contrast, most amino acids, organic acids, and other small molecules are concentrated near the origin, indicating that their contributions to the overall variance are more moderate. This pattern of loadings underscores the central role of sugar metabolism and amine-related metabolites in shaping the differences between species and treatments observed in the scores plot (Fig. 1b).

The cluster analysis, built using Euclidean distances and the Ward algorithm, broadly confirms the groupings suggested by the PCA (Fig. 1c). The first major split separates *A. diaperinus* from *T. molitor*, mirroring the distinction along PC1 in the scores plot. Within each species, the samples then form subclusters according to the three treatments, control, EO, and pirimiphos-methyl, which is consistent with the treatment-based separation observed along PC2 in the PCA.

The comprehensive analysis using PCA has provided an unbiased view of the overall data structure, revealing clear interspecies differences and treatment effects. Moving forward with a PLS-DA analysis on a single species allowed us to specifically target and enhance the

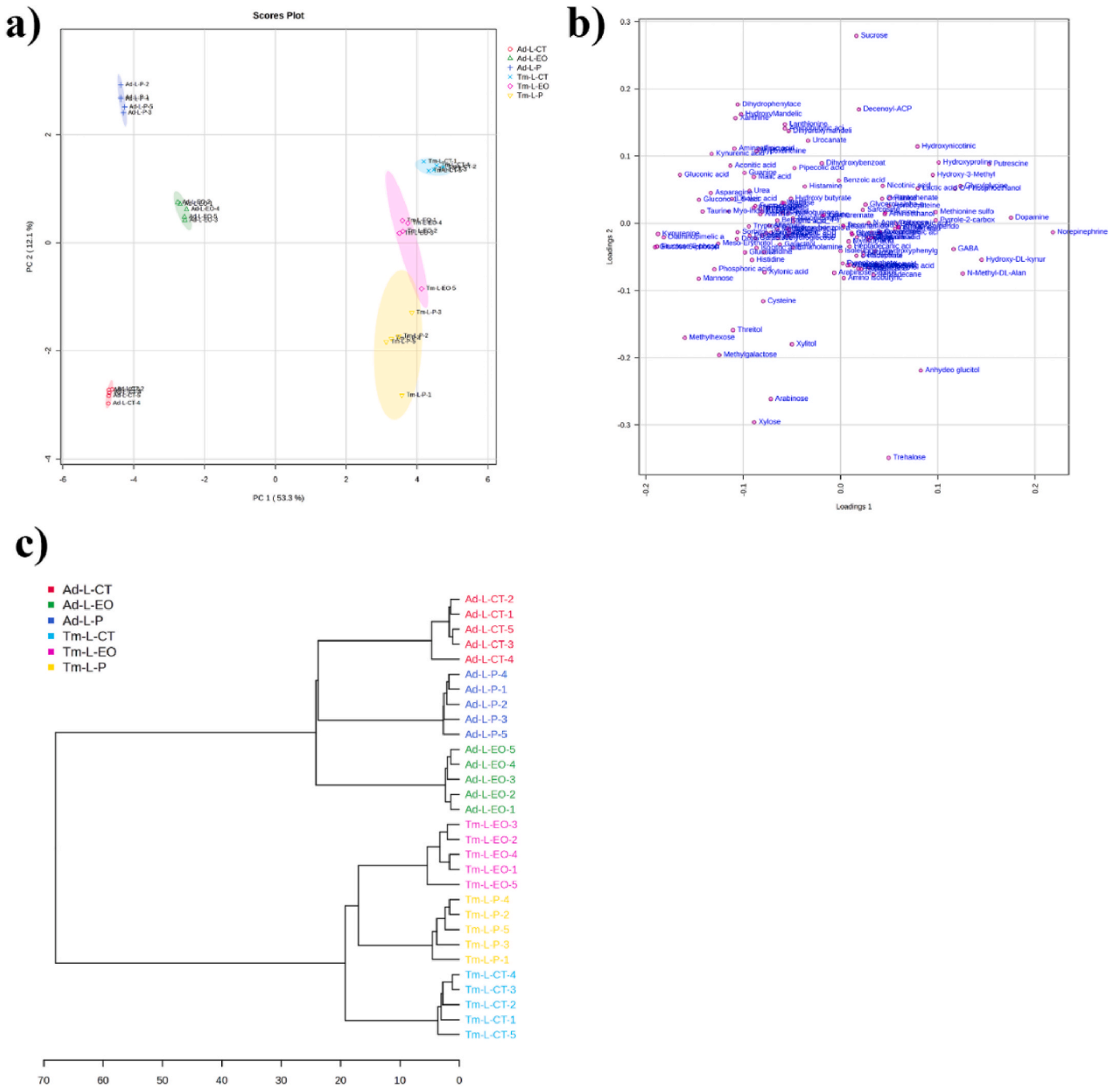

Fig. 1. Multivariate Principal Component Analysis (PCA) of the metabolic profiles of the larval stage (L) of *Alphitobius diaperinus* (Ad) and *Tenebrio molitor* (Tm) treated with *Commiphora myrrha* essential oil (EO), the insecticide pirimiphos-methyl (P) and control (CT). (a) PCA scores plot displaying the separation of metabolic profiles across the six experimental groups (Tm-L-CT, Tm-L-EO, Tm-L-P and Ad-L-CT, Ad-L-EO, Ad-L-P). (b) The PCA loadings plot illustrates the contribution of individual metabolites to the separation observed in the scores plot. Metabolites further from the origin have a stronger impact on group differentiation. (c) Hierarchical clustering dendrogram, built using the Euclidean distance and Ward as clusterizing algorithm, showing the relationships between individual samples based on metabolic similarity. For improved readability, a high-resolution version of this figure is available in Table S1. N = 5.

separation between treatment groups. This supervised approach is expected to uncover finer, species-specific metabolic changes, thereby complementing and deepening the insights gained from the wider analysis.

The PLS-DA analysis for each species clearly differentiates the treatment groups (Fig. 2a–c) by emphasizing key metabolites with VIP scores above 1.4. In *A. diaperinus*, the VIP plot and its associated heatmap reveal that metabolites such as sugars and sugar alcohols (e.g., trehalose, arabinose, xylose, mannose, xylitol, threitol) were significantly down-produced compared to control in both EO and pirimiphos-methyl treatments. Conversely, energy-related sugars, phenolic compounds, amino acid derivatives, lipid intermediates, and nitrogenous bases (including sucrose, dihydroxyphenylacetic acid, aminoadipic acid, decanoyl-ACP, putrescine, and xanthine), were markedly accumulated in the insecticide treatment (Fig. 2b). In *T. molitor*, EO treatment led to an increase in glycolytic and pentose phosphate intermediates (e.g., trehalose, xylose, glucose-6-phosphate, fructose-6-phosphate), and a reduction in amino acids and carboxylic acids (e.g., hydroxyproline, nicotinic acid, lactic acid) (Fig. 2d). These consistent patterns suggest that although EO and pirimiphos-methyl may act via different

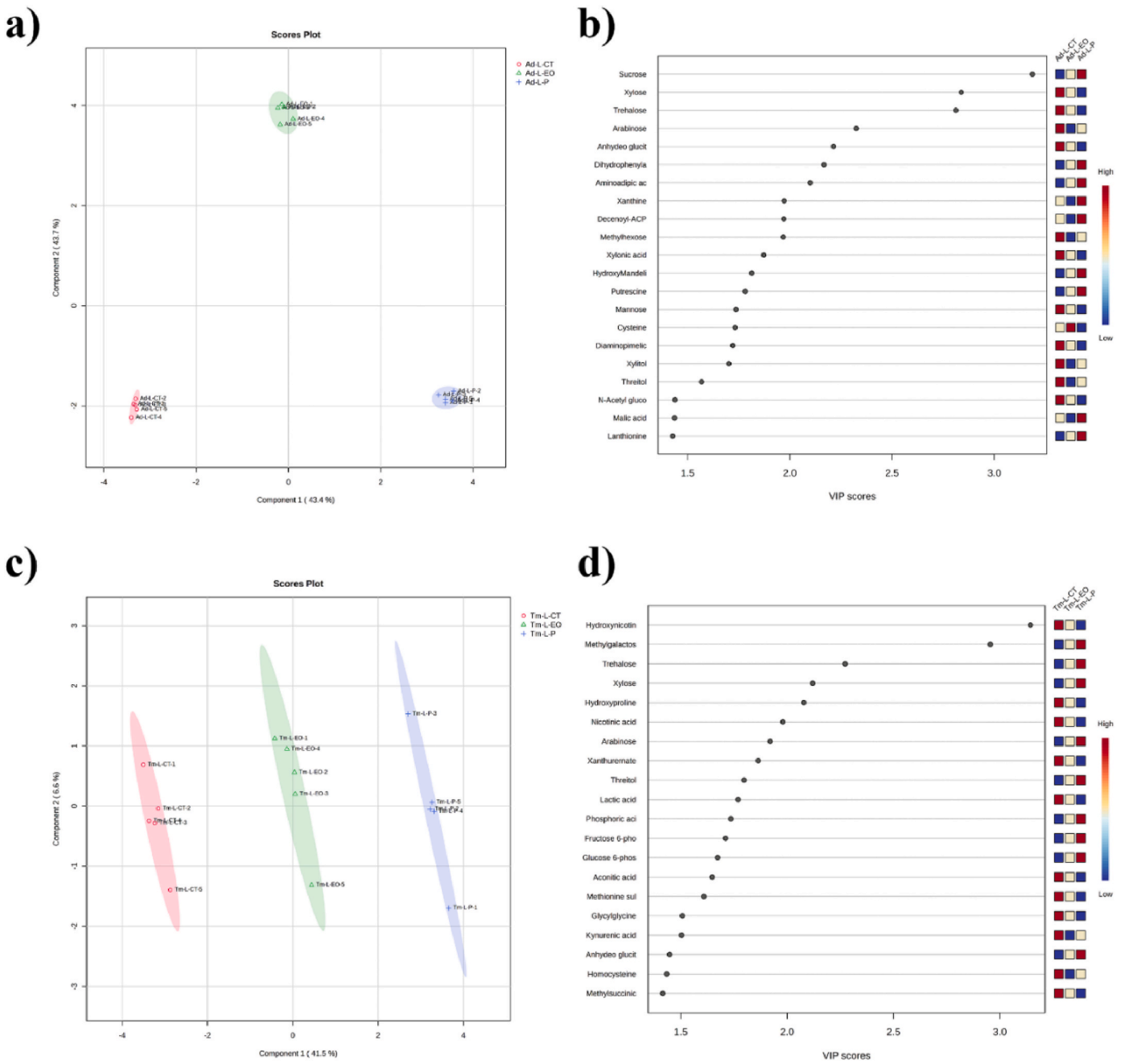

Fig. 2. Multivariate Partial Least Square Discriminant Analysis (PLS-DA) of the larval stage (L) of *Alphitobius diaperinus* (Ad) and *Tenebrio molitor* (Tm) treated with *Commiphora myrrha* essential oil (EO), the insecticide pirimiphos-methyl (P) and control (CT). (a) *Alphitobius diaperinus* PLS-DA scores plot displaying the separation of metabolic profiles across the six experimental groups (Ad-L-CT, Ad-L-EO, Ad-L-P). (b) PLS-DA VIP scores built on *A. diaperinus* data illustrate individual metabolites' contribution to the separation observed in the scores plot. (c) *Tenebrio molitor* PLS-DA scores plot displaying the separation of metabolic profiles across the six experimental groups (Tm-L-CT, Tm-L-EO, Tm-L-P). (c) PLS-DA VIP scores built on *T. molitor* data illustrate individual metabolites' contribution to the separation observed in the scores plot. For improved readability, a high-resolution version of this figure is available in Table S1. N = 5.

mechanisms, they elicit comparable metabolic shifts in each species. Model robustness was validated via permutation tests and cross-validation, supporting the biological relevance of the results (see Table S1).

Following multivariate analysis, univariate ANOVA was used to identify all metabolites significantly affected by treatments in both species. The top 60 altered metabolites were visualized using heatmaps, with hierarchical clustering on the left side organizing them by profile similarity (Fig. 3a and b).

In *A. diaperinus*, amino acids, organic acids, and sugar-related metabolites (e.g., asparagine, tryptophan, alanine, fructose, lactic acid, aconitic acid, isocitric acid) were generally reduced under EO treatment, while pirimiphos-methyl caused their accumulation. A second cluster of polyols and sugar phosphates (e.g., inositol, galactinol, glucose-6-phosphate, fructose-6-phosphate) showed a shared downregulation under both treatments. Additionally, a treatment-specific cluster included polyamines, fatty acid intermediates, and purine metabolites (e.g., putrescine, decanoyl-ACP, aminoadipic acid, xanthine, hypoxanthine, urocanate), all elevated exclusively in the pirimiphos-methyl group (Fig. 3a).

In *T. molitor*, the EO treatment caused an increase in neuroactive compounds and glycerol-related metabolites (e.g., xanthine, glycerol,

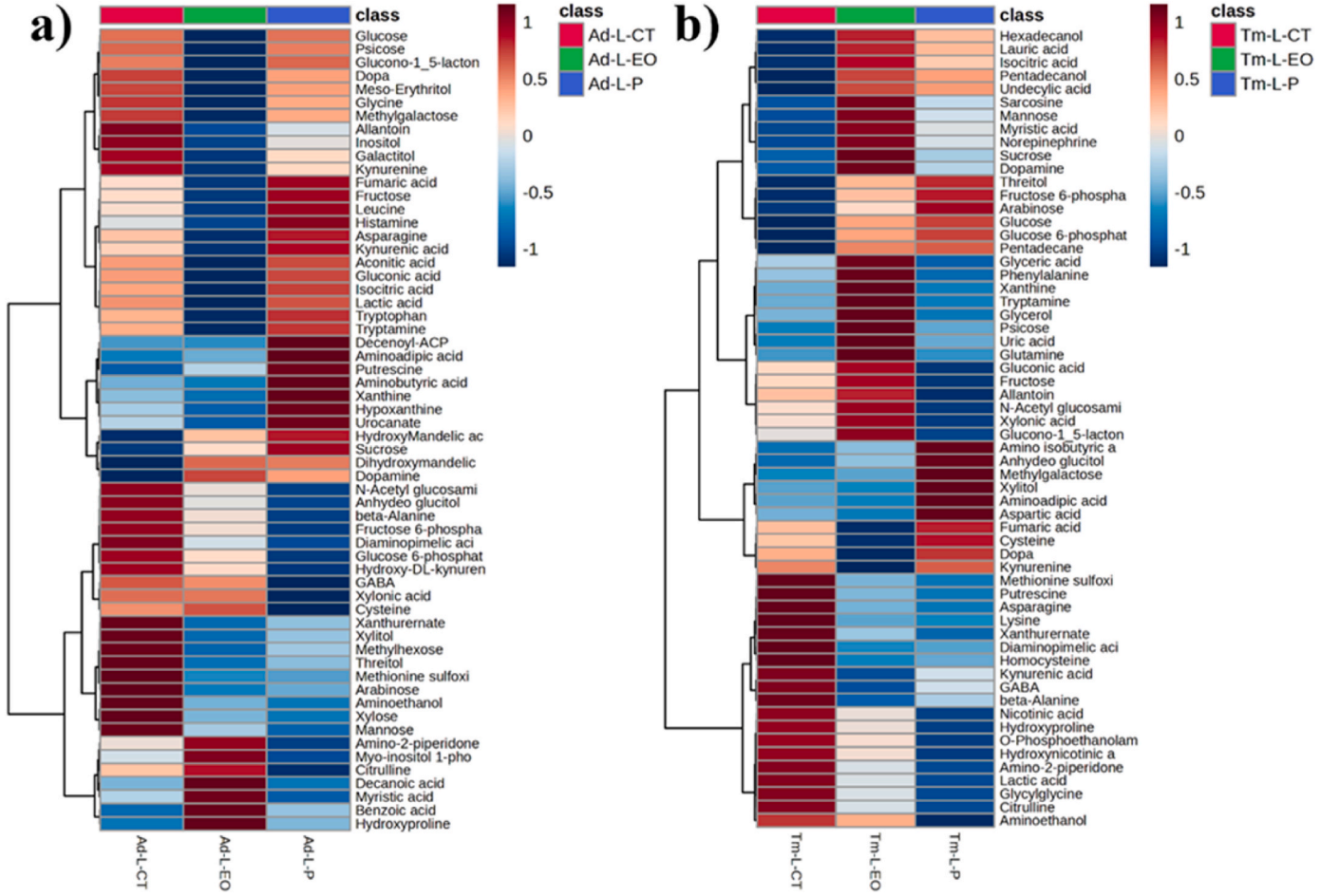

Fig. 3. Top 60 metabolites resulting from the one-way ANOVA are reported as a clusterised heatmap in a) the larval stage (L) of *Alphitobius diaperinus* (Ad) and b) *Tenebrio molitor* (Tm) treated with *Commiphora myrrha* essential oil (EO), the insecticide pirimiphos-methyl (P) and control (CT). The top hierarchical clusterization was built using the Euclidean distance and Ward as clusterizing algorithm. For improved readability, a high-resolution version of this figure is available in Supplementary Table S1. N = 5. The full list of significantly altered metabolites resulting from the ANOVA is reported in Table S1.

tryptamine, glyceric acid), while several oxidized sugar derivatives (e.g., gluconic acid, xylonic acid, N-acetylglucosamine) were elevated in EO and suppressed in insecticide-treated larvae (Fig. 3b). A separate cluster, rich in amino acid catabolites and tryptophan-derived compounds (e.g., diaminopimelic acid, xanthurenate), decreased in both treatments. A final set of methylated sugars and polyols increased under insecticide exposure, while core sugars (e.g., threitol, glucose, glucose-6-phosphate, arabinose) rose under both treatments (Fig. 3b).

The four DSPC networks in Fig. 4 reveal a consistent pattern: pirimiphos-methyl treatment leads to tighter, denser metabolite correlations, while *C. myrrha* EO results in more fragmented networks (Fig. 4a–d). In both *A. diaperinus* and *T. molitor*, EO-treated larvae show two or three isolated clusters linked by mostly negative edges (Fig. 4a–c), whereas pirimiphos-methyl forms one large module in *A. diaperinus* and two densely connected clusters in *T. molitor* (Fig. 4b–d).

In *A. diaperinus* under EO, the network centers on carbohydrate and sugar alcohol metabolism, with glucose and sucrose being the most connected metabolites (degree = 12) and displaying the highest betweenness values (124.31 and 120.72). Meso-erythritol (degree = 10), psicose (degree = 9, betweenness = 57.92), xylitol (68.41), and fructose (35.53) also play key roles. Additionally, kynurenine (degree = 10) and dopa (degree = 9) suggest modulation of tryptophan and tyrosine pathways (Fig. 4a–Table S2).

Under pirimiphos-methyl, *A. diaperinus* exhibits a broader network. Xylose (degree = 16) and cysteine (degree = 15, highest betweenness = 28.46) dominate, with significant contributions from aminoadipic acid, methylhexose, and putrescine (each degree = 15), implicating lysine, sugar, and polyamine metabolism. Xanthine (degree = 14, betweenness = 53.85) reflects purine pathway involvement. Sucrose, methylgalactose, and arabinose (all degree = 14), as well as decanoyl-ACP (degree = 10, betweenness = 62.01), underscore effects on sugar and fatty acid metabolism (Fig. 4b–Table S3).

In *T. molitor* treated with EO, the network shifts toward neurotransmitter and energy metabolism. Beta-alanine and norepinephrine are the most connected nodes (degree = 14), with beta-alanine also showing high betweenness (58.65). Isocitric acid stands out with the highest centrality overall (degree = 11, betweenness = 112.44), while dopamine and uric acid (both degree = 11, betweenness = 16.65) indicate roles in redox balance (Fig. 4c–Table S4).

Under pirimiphos-methyl, *T. molitor* shows a distinct configuration. Hydroxynicotinic acid and methylgalactose are the most connected metabolites (degree = 15), with the former also having the highest betweenness (50.06), indicating oxidative stress involvement. Xanthurernate (degree = 14, betweenness = 28.91) reflects tryptophan catabolism. O-phosphoethanolamine (degree = 13, betweenness = 21.19) and putrescine (degree = 13, betweenness = 19.20) highlight changes in phospholipid metabolism and polyamine pathways (Fig. 4d–Table S5).

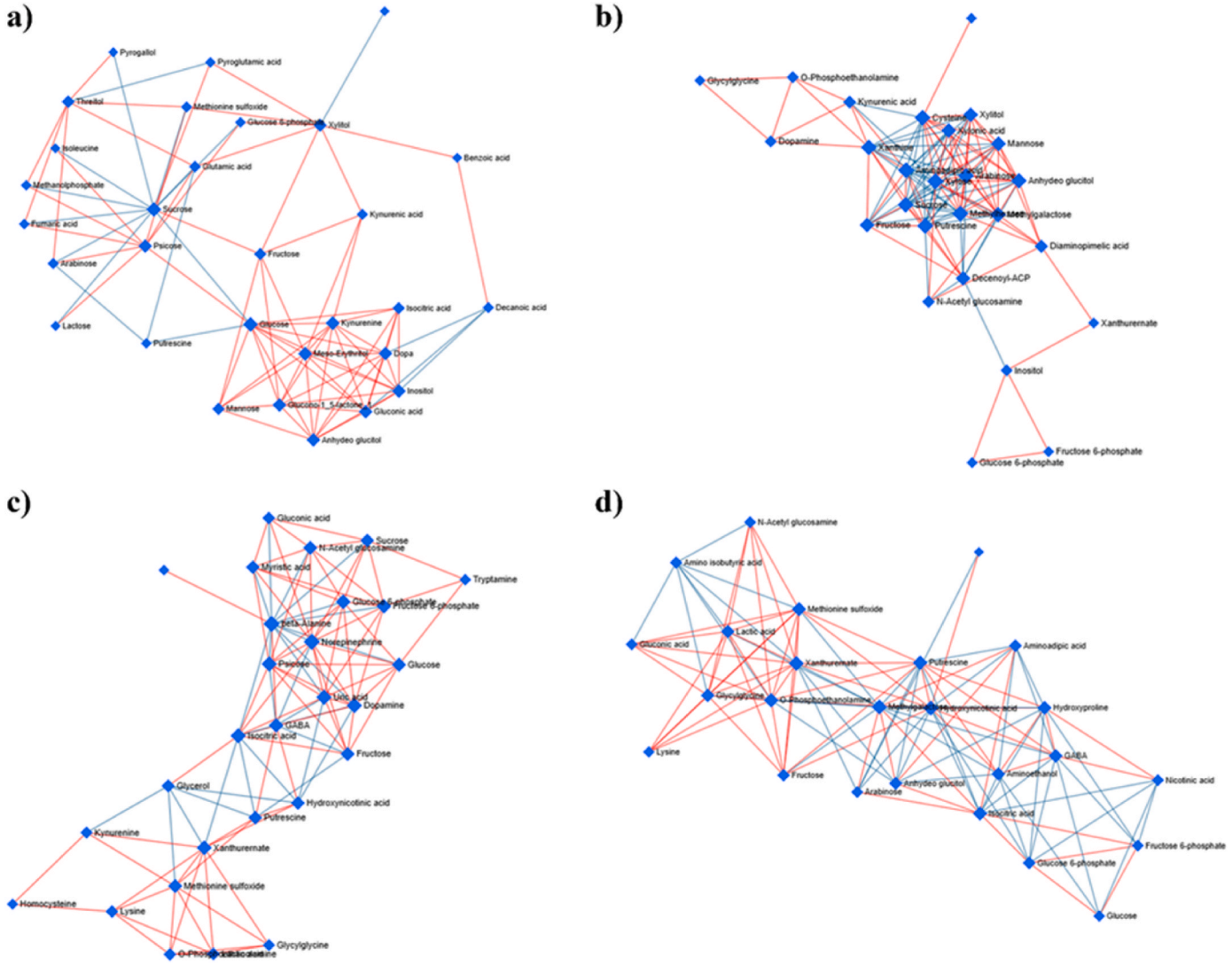

Fig. 4. Correlation network obtained by DSPC algorithm using the metabolites identified in the larval stage of *Alphitobius diaperinus* treated with *Commiphora myrrha* essential oil (EO) (a) and the insecticide pirimiphos-methyl (b), and those identified in *Tenebrio molitor* treated with *C. myrrha* EO (c) and the insecticide pirimiphos-methyl (d). Blue nodes represent metabolites, red lines indicate a positive correlation between metabolites, and blue lines indicate a negative correlation. For improved readability, a high-resolution version of this figure is available in Table S1. N = 5. (For interpretation of the references to colour in this figure legend, the reader is referred to the Web version of this article.)

3.6. Effects of C. myrrha EO on A. diaperinus and T. molitor adult metabolome

The PCA score plot highlights that the first two principal components together explain a substantial portion of the total variance (about 62 %, with PC1 at 45.7 % and PC2 at 16.45 %). Along the horizontal axis (PC1), the two insect species occupy distinctly different regions: *A. diaperinus* appears predominantly on the negative side, while *T. molitor* is on the positive side. This separation along PC1 suggests that inherent species-level differences strongly influence the measured parameters (Fig. 5a).

Within each species, the three treatment groups, control , EO, and pirimiphos-methyl, also form distinct clusters, indicating that both the myrrh EO and the commercial insecticide elicit characteristic responses. For *A. diaperinus*, the EO-treated group (Ad-A-EO) clusters toward the top-left portion of the plot (negative PC1, positive PC2), whereas the control (Ad-A-CT) and the pirimiphos-treated group (Ad-A-P) lie in other quadrants. This pattern highlights a pronounced shift from the control condition when the insects are exposed to either the EO or the insecticide, with the EO cluster showing particularly strong separation along PC2 (Fig. 5a).

A similar pattern of distinct clustering appears in *T. molitor*, although its data points are shifted to the positive side of PC1. The *T. molitor* control group (Tm-A-CT) occupies the lower-right portion of the plot (positive PC1, negative PC2), the pirimiphos-treated group (Tm-A-P) remains nearby in the same general quadrant, and the EO-treated group (Tm-A-EO) appears higher along PC2 in the upper-right region. Thus, for both species, the *C. myrrha* EO at the ED_{50} concentration creates a response profile that sets it apart from the conventional insecticide treatment. Overall, the PCA underscores that each treatment, be it the natural EO or the synthetic insecticide, leads to distinct biological or biochemical changes, and that these differences are clearly visible when the data are reduced to the first two principal components (Fig. 5a).

In the loadings plot, the metabolites located farthest from the origin along PC1 and PC2 are the main drivers of the separation observed in the score plot. On the negative side of PC1, a cluster of aromatic and phenolic compounds, including hydroquinone derivatives, simple phenols, and catecholamines, exerts a pronounced influence (Fig. 5b). In contrast, the positive side of PC1 is more closely associated with carbohydrates and amino acids, suggesting a metabolic shift toward

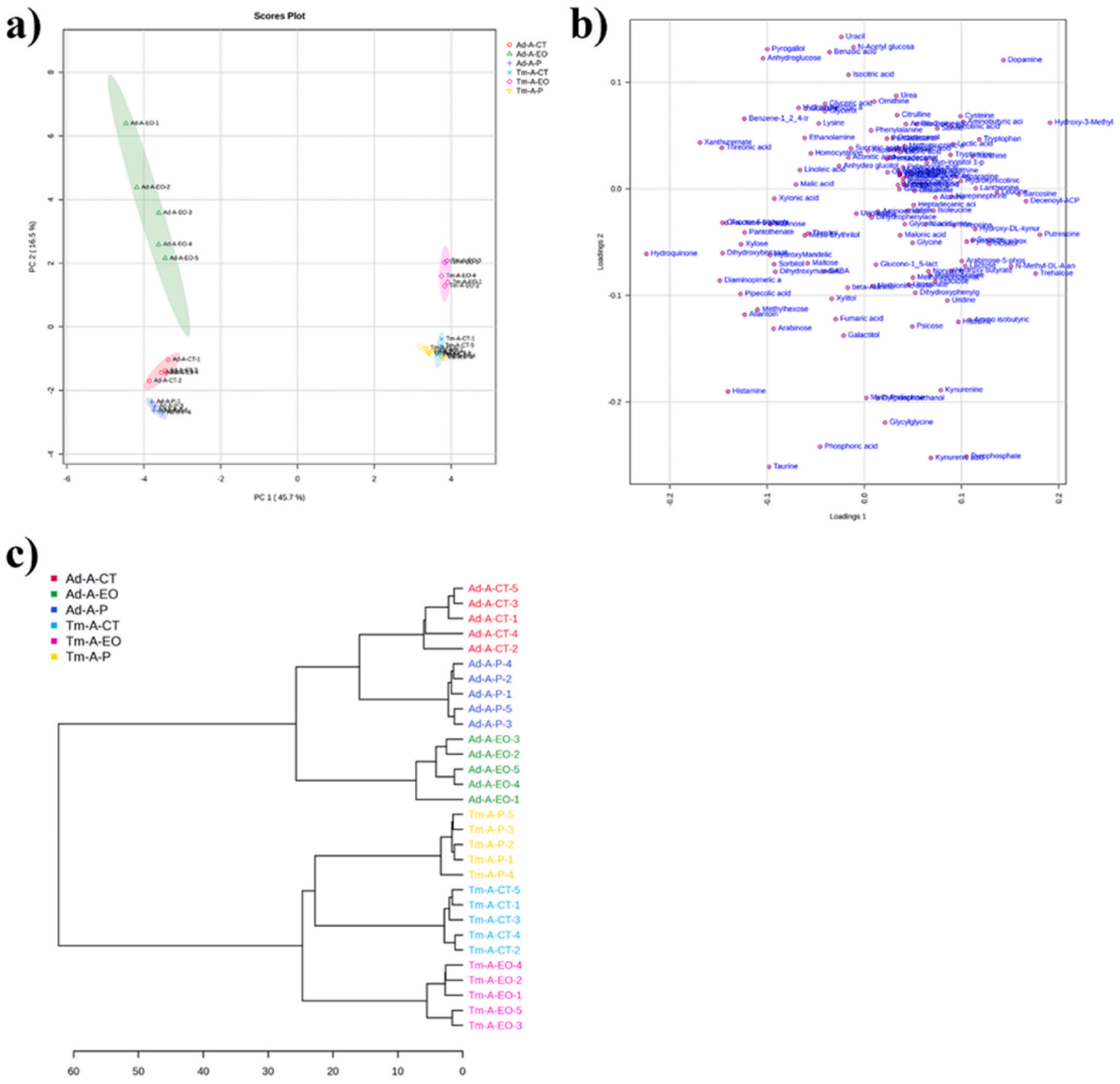

Fig. 5. Multivariate Principal Component Analysis (PCA) of the metabolic profiles of the adult stage (A) of *Alphitobius diaperinus* (Ad) and *Tenebrio molitor* (Tm) treated with *Commiphora myrrha* essential oil (EO), the insecticide pirimiphos-methyl (P) and control (CT). (a) PCA scores plot displaying the separation of metabolic profiles across the six experimental groups (Tm-A-CT, Tm-A-EO, Tm-A-P and Ad-A-CT, Ad-A-EO, Ad-A-P). (b) The PCA loadings plot illustrates the contribution of individual metabolites to the separation observed in the scores plot. Metabolites further from the origin have a stronger impact on group differentiation. (c) Hierarchical clustering dendrogram, built using the Euclidean distance and Ward as clusterizing algorithm, showing the relationships between individual samples based on metabolic similarity. For improved readability, a high-resolution version of this figure is available in Table S1. N = 5.

energy-related pathways (Fig. 5b).

Along PC2, higher loadings are driven by sulfur- and nitrogen-containing compounds such as cysteine, cystine, and tryptophan. In comparison, lower loadings are associated with amines and nitrogenous metabolites involved in neurotransmission and immune response, including histamine, taurine, and kynurenine (Fig. 5b).

This distribution indicates that variation in phenolic and aromatic metabolism underlies much of the separation along PC1, whereas amino acid profiles, nitrogen metabolism, and organic acid levels are more influential along PC2. The positioning of sugar-related metabolites on the positive side of PC1 further supports the contribution of carbohydrate metabolism to species and treatment differentiation.

The hierarchical cluster analysis using Euclidean distances and Ward's algorithm reveals two main branches that clearly separate *A. diaperinus* from *T. molitor*, mirroring the species-level distinctions seen in the PCA score plot (Fig. 5c). Within each species branch, the samples form well-defined subclusters according to the three treatments, control, EO, and pirimiphos-methyl, indicating that the metabolic profiles of insects under each condition are sufficiently distinct to group together (Fig. 5c). Overall, this clustering pattern corroborates the PCA

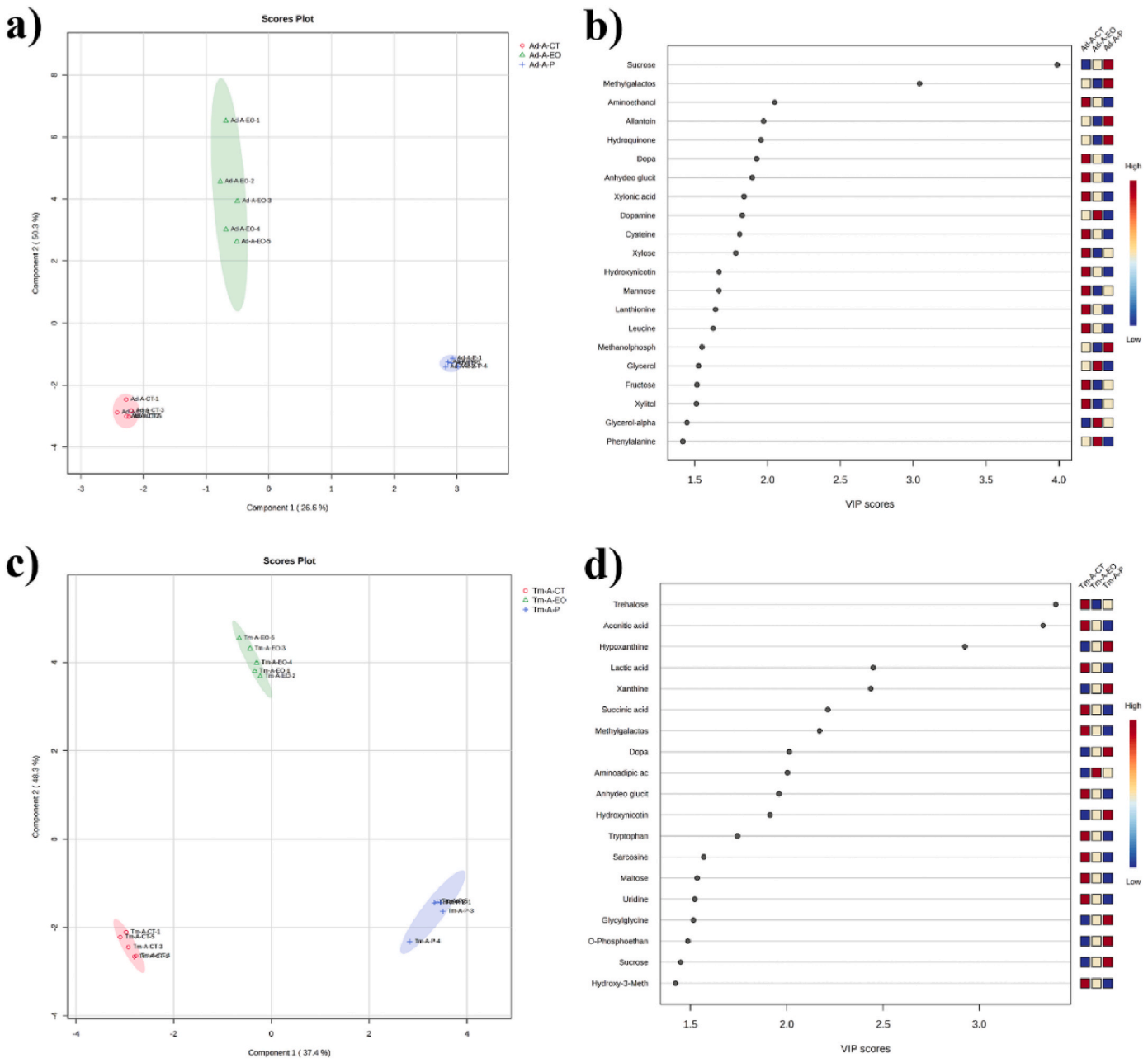

Fig. 6. Multivariate Partial Least Square Discriminant Analysis (PLS-DA) of the adult stage (A) of *Alphitobius diaperinus* (Ad) and *Tenebrio molitor* (Tm) treated with *Commiphora myrrha* essential oil (EO), the insecticide pirimiphos-methyl (P) and control (CT). (a) *Alphitobius diaperinus* PLS-DA scores plot displaying the separation of metabolic profiles across the six experimental groups (Ad-A-CT, Ad-A-EO, Ad-A-P). (b) PLS-DA VIP scores built on *A. diaperinus* data illustrate individual metabolites' contribution to the separation observed in the scores plot. (c) *Tenebrio molitor* PLS-DA scores plot displaying the separation of metabolic profiles across the six experimental groups (Tm-A-CT, Tm-A-EO, Tm-A-P). (c) PLS-DA VIP scores built on *T. molitor* data illustrate individual metabolites' contribution to the separation observed in the scores plot. For improved readability, a high-resolution version of this figure is available in Table S1. N = 5.

findings by confirming that both species identity and the nature of the treatment drive the main differences in their metabolic responses (Fig. 5).

As previously done, data for adults were also further analyzed through PLS-DA, carried out on the single species, to uncover finer, species-specific metabolic changes and complement PCA data. The PLS-DA score plots built on both species further confirmed the separation observed among all treatments, suggesting that the EO and the commercial insecticide differ in their effect on *A. diaperinus* and *T. molitor* metabolism (Fig. 6a–c)

In the PLS-DA models for both insect species, the VIP scores identified key discriminatory metabolites that differentiate treatment groups. In *A. diaperinus*, the highest VIP values were associated with a combination of sugars, methylated carbohydrates, nitrogen-containing compounds, and aromatic or phenolic metabolites, including representatives from polyol metabolism and catecholamine pathways (Fig. 6b).

A similar metabolic signature was observed in *T. molitor*, where group separation was likewise driven by carbohydrates, methylated sugars, nitrogenous intermediates, and phenolic compounds involved in redox and neurotransmitter pathways (Fig. 6d).

In both adult species, the top 60 metabolites identified through ANOVA were visualized as heatmaps (Fig. 7a and b), revealing treatment- and species-specific patterns. These included metabolites showing consistent trends across species as well as others displaying contrasting

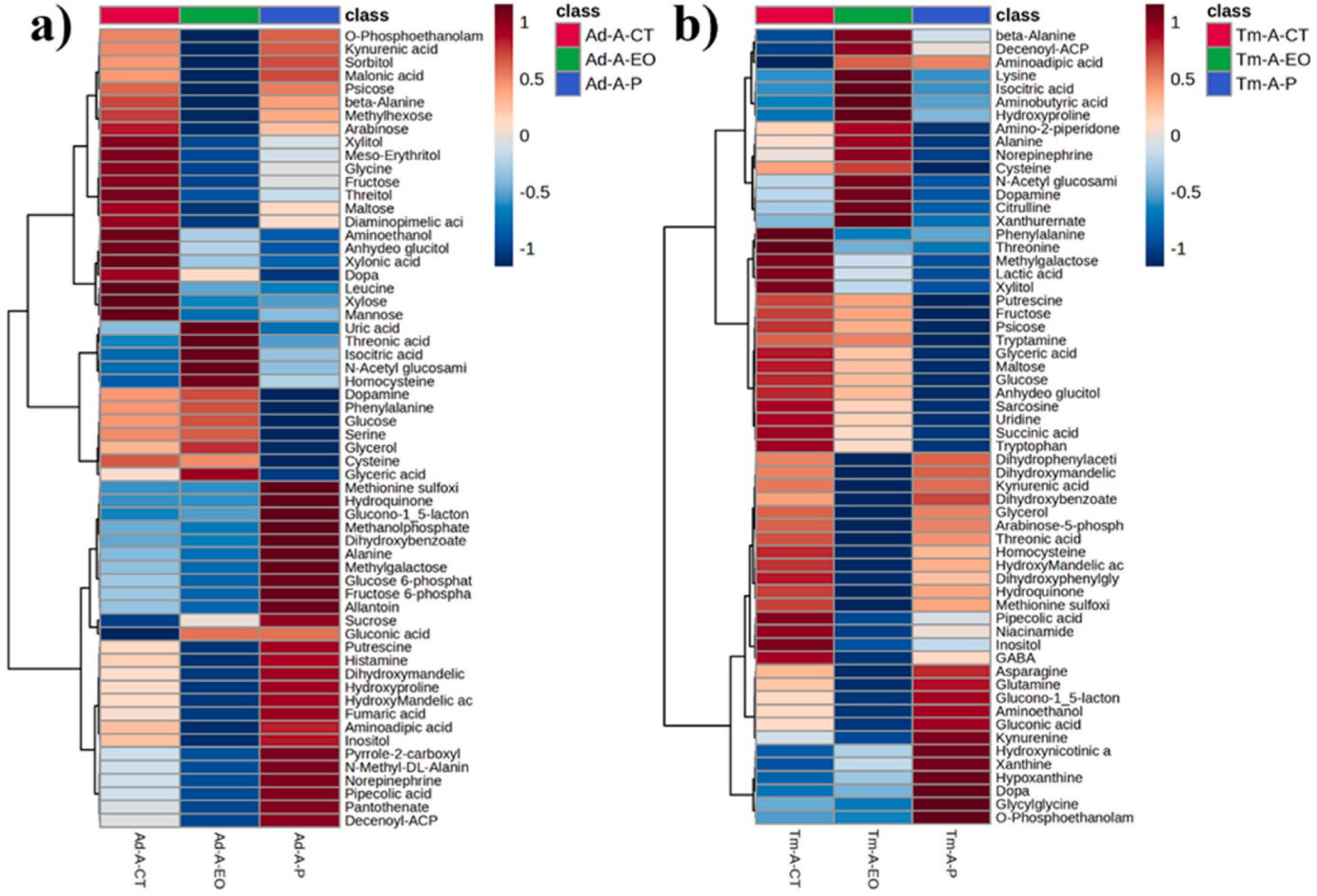

Fig. 7. Top 60 metabolites resulting from the one-way ANOVA are reported as a clustered heatmap in a) the adult stage (A) of *Alphitobius diaperinus* (Ad) and b) *Tenebrio molitor* (Tm) treated with *Commiphora myrrha* essential oil (EO), the insecticide pirimiphos-methyl (P) and control (CT). The top hierarchical clusterization was built using the Euclidean distance and Ward as clusterizing algorithm. For improved readability, a high-resolution version of this figure is available in Supplementary Table S1. N = 5. The full list of significantly altered metabolites resulting from the ANOVA is reported in Table S1.

responses, further emphasizing the distinct metabolic reprogramming induced by each treatment (Fig. 7a and b).

Debiased sparse partial correlation network analysis in *A. diaperinus* and *T. molitor* adults, following treatment with either *C. myrrha* EO or the commercial insecticide pirimiphos-methyl, revealed distinct species- and treatment-specific metabolic reprogramming patterns (Fig. 8a–d; Table S6–S9).

In *A. diaperinus* adults, EO treatment generated a moderately dense and modular network, with clustering primarily around carbohydrate-related metabolites (Fig. 8a). Xylitol emerged as the central hub (degree = 16; betweenness = 87.33), with psicose (degree = 13) and arabinose (degree = 11) also highly connected, indicating significant alterations in sugar metabolism. Additionally, stress-related metabolites, such as hydroxyproline and histamine, showed elevated connectivity, suggesting involvement in oxidative stress responses (Table S6).

In contrast, pirimiphos-methyl treatment produced a highly interconnected and complex network (Fig. 8b). Methylgalactose was the most connected metabolite (degree = 21; betweenness = 55.38), followed by histamine (degree = 19; betweenness = 41.06), highlighting their central roles. The network also featured key nodes from amino acid and sugar metabolism, reflecting broad biochemical disruption (Table S7).

In *T. molitor*, EO treatment resulted in a less dense and more compartmentalized network (Fig. 8c). Several metabolites, including citrulline, methionine sulfoxide, dihydroxymandelic acid, and methylgalactose (each degree = 13), were among the most connected. Beta-alanine also emerged as a central node, pointing to the modulation of amino acid metabolism and stress adaptation (Table S8).

Under pirimiphos-methyl exposure, the network in *T. molitor* was fragmented, with methylgalactose and lactic acid (each degree = 13) among the most connected (Fig. 8d). Notably, O-phosphoethanolamine displayed the highest betweenness centrality (129.93), indicating a major role in phospholipid metabolism and membrane regulation. Other important contributors included fructose and aminoadipic acid, reinforcing the impact on energy and nitrogen metabolism (Table S9).

4. Discussion

The chemical composition of myrrh EO analyzed in this study was quite similar to those reported in literature. For instance, Dekebo et al. (2002), Marongiu et al. (2005), and Spinozzi et al. (2025) reported furanoeudesma-1,3-diene and lindestrene among major constituents, accounting for 34–41.40 and 12–14 % of the total EO composition, respectively. However, major differences were found in terms of isofuranodiene content between this study and those of Marongiu et al. (2005) and Morteza-Semnani and Saeedi (2003), who did not detect this compound. It is worthy to consider that GC-MS analysis is not the most appropriate technique for its quantification. In fact, this molecule usually undergoes Cope rearrangement when subjected to high temperatures being subsequently converted into curzerene (Baldovini et al., 2001; Maggi et al., 2012; Spinozzi et al., 2025). Thus, to overcome this problem and to produce reliable results, the furanoeudesma-1,3-diene,

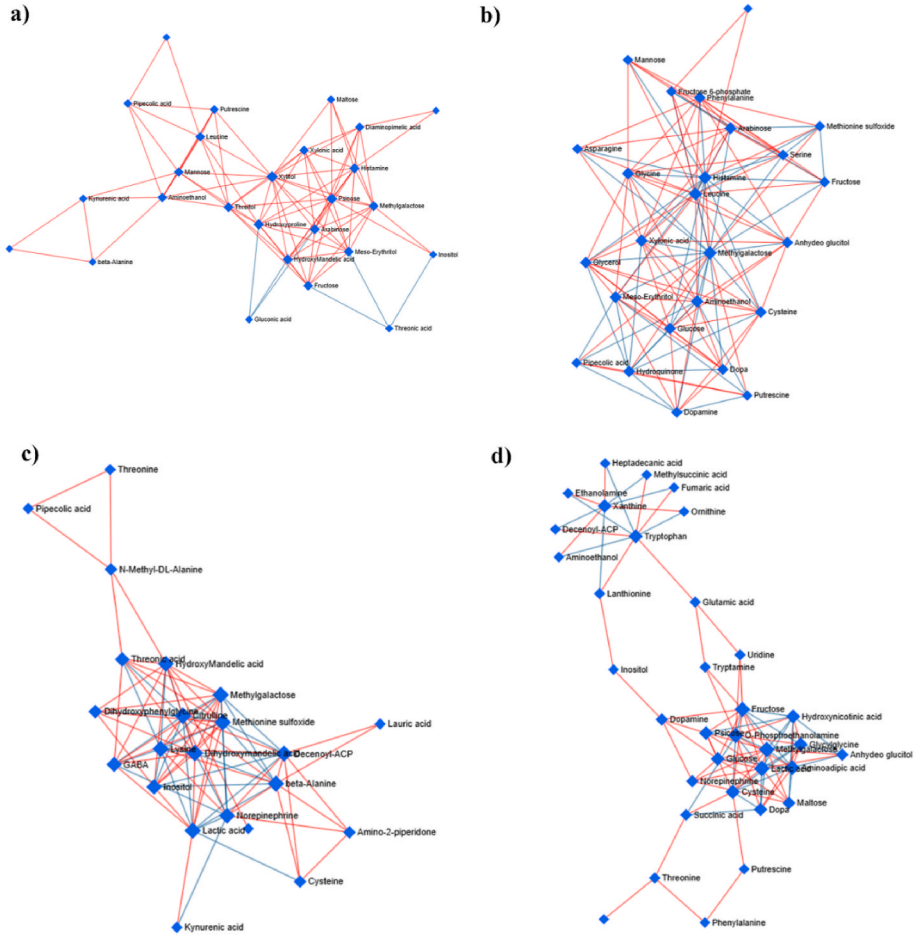

Fig. 8. Correlation network obtained by DSPC algorithm using the metabolites identified in the adult stage of *Alphitobius diaperinus* treated with *Commiphora myrrha* essential oil (EO) (a) and the insecticide pirimiphos-methyl (b), and those identified in *Tenebrio molitor* treated with *C. myrrha* EO (c) and the insecticide pirimiphos-methyl (d). Blue nodes represent metabolites, red lines indicate a positive correlation between metabolites, and blue lines indicate a negative correlation. For improved readability, a high-resolution version of this figure is available in Table S1. N = 5. (For interpretation of the references to colour in this figure legend, the reader is referred to the Web version of this article.)

isofuranodiene, and curzerene content in myrrh EO was determined through HPLC-DAD analysis. Since the latter confirmed the data of the semi-quantitative analysis carried out with the GC-MS, it is highly likely that the Cope rearrangement of isofuranodiene occurred during the hydrodistillation of the EO from the myrrh oleo-gum resin, being this process performed at high temperatures (Spinozzi et al., 2025).

It is noteworthy that the EO assays, especially at the highest concentration, proved to be highly effective against *T. molitor* larvae. The latter appeared to be susceptible to monoterpene compounds, like eugenol, generally found in cinnamon and clove EO according to Martínez et al. (2018). Nevertheless, prior research has shown that adults of *T. molitor* demonstrated susceptibility to various plant secondary metabolites like 2-undecanone, *trans*-anethole, acetic acid, (*E*)-2-decenal, and (*E,E*)-2,4-decadienal, and furfural in comparison to their larval counterparts (Ntalli et al., 2021). In studies that evaluated the efficacy of various EOs against *T. molitor* adults and larvae, results showed that larvae were notably more tolerant if compared to the adults (Kavallieratos et al., 2024a, 2024b, 2025). The promising results of the insecticidal effectiveness of myrrh EO is also highlighted by the fact that even synthetic insecticides are inefficient against *T. molitor* larvae (Athanassiou et al., 2015; Kavallieratos et al., 2019, 2021; Pedersen et al., 2020). This varying response to natural substances with insecticidal properties may be due to the different cuticular composition among the developmental stages (Mewis and Ulrichs, 2001), as well as the variation in the insecticidal uptake from the cuticle of each stage (Pedersen et al., 2020). Moreover, the mechanism of action of the compounds could also be responsible for the difference detected between the two developmental stages. Although that of myrrh EO is still unclear, it has been reported that the lipophilicity and volatility of furanosesquiterpenes, specifically of isofuranodiene, enhance their absorption in the insect body and their fumigant effects, thus increasing the toxicity (Benelli et al., 2017; Perumalsamy et al., 2009). Therefore, this study showed that each EO, when applied as grain protectant, owns a specific mechanism of action on life stages of *T. molitor* depending on its peculiar phytochemical composition. It is hypothesized that different EOs could be used for the targeted green management of *T. molitor*, according to the prevailing life stage (Ntalli et al., 2021).

Results indicated that both adults and larvae of *A. diaperinus* were susceptible to myrrh EO, suffering high mortalities (> 86 % and > 91 %, respectively) when exposed to a concentration of 1000 ppm. These findings make this product a promising ally for the control of this species. In contrast, EOs from other plant species were not effective against *A. diaperinus* when applied on grains (Velusamy et al., 2020; Kavallieratos et al., 2024a, 2024b, 2025). For instance, EOs from *Eucalyptus globulus* Labill. and *Cymbopogon citratus* (DC.) Stapf did not yield any mortality of neither adults, nor larvae of *A. diaperinus*, even at high concentrations (20 %) (Velusamy et al., 2020). Additionally, 1000 ppm of *Juniperus* × *pfitzeriana* (Späth) P.A.Schmidt and *Hesperocyparis*

arizonica (Greene) Bartel EOs resulted in 4.4 and 11.1 % mortality of *A. diaperinus* adults, respectively, while in 10 and 0 % mortality of *A. diaperinus* larvae, respectively (Kavallieratos et al., 2024a). A similar trend was observed for *Crithmum maritimum* L. and *Xylopia aethiopica* (Dunal) A.Rich. achieving 13.3 and 44.4 %, or 53.3 and 5.6 % mortalities of *A. diaperinus* adults and larvae, respectively, after 7 days of exposure at 1000 ppm (Kavallieratos et al., 2024a, 2025). The notable effectiveness of the myrrh EO, if compared to other EOs, against different developmental stages of *A. diaperinus*, reveals its elevated potential to be used in pest management, alone or as a component of insecticide formulations.

The results of the current study are consistent with those of previous research examining the insecticidal effectiveness of EO or extracts of *C. myrrha* against other important insect species. Alanazi et al. (2024) supported that methanol extracts derived from the resin of *C. myrrha* provided elevated efficacy against larvae and pupae of *A. aegypti*. Toxicity increased in a concentration-dependent manner as exposure time prolonged (95 and 98.33 % for larvae and pupae, respectively). In a recent study, Spinozzi et al. (2025) reported notably low myrrh EO LC_{50} values, ranging from 4.42 to 16.80 μg/mL, against four mosquito species: *Ae. aegypti*, *Aedes albopictus* (Skuse), *Anopheles stephensi* Liston, and *Anopheles gambiae* Giles (Diptera: Culicidae). Furthermore, Al-Fuhaid (2017) found that methanol extracts from *C. myrrha* resulted in complete larval mortality of *T. granarium*.

While this study provides valuable insights into the insecticidal potential of *C. myrrha* EO, further research is required to optimize its application in commercial stored-product protection. Future efforts could explore different formulations to enhance the stability and efficacy of the EO, as well as different methods of application to different species of insects and their respective life stages. Moreover, it could be important to provide more information on the biochemical and physiological mechanisms underlying insect susceptibility to this product. Our findings align with previous research on the insecticidal properties of *C. myrrha* EO and its compounds such as isofuranodiene (Pavela et al., 2019), reinforcing its use as a viable component of integrated pest management in stored-product protection. The industrial exploitation of myrrh EO could be favored by the already established applications of the oleo-gum resin in herbal products, foods, cosmetics, and pharmaceuticals (Leung and Foster, 1996). Moreover, the economic feasibility of its commercial development is enhanced by the relatively low price of myrrh on the market (11.00–15.00 $/kg) (Lubbe and Verpoorte, 2011) making it suitable for a large-scale EO production. However, additional challenges like non-target effects, environmental safety, and potential impacts on grain quality will need to be overcome to ensure the feasibility of these plants EO as practical solution to large scale protection of storage units.

The EO-treated *A. diaperinus* larvae displayed extensive carbohydrate and sugar alcohol metabolism shifts, with glucose and sucrose as central hubs, similar to metabolic effects reported for insecticides like imidacloprid, permethrin, and malathion (Mansingh, 1965; Cotton and Anstee, 1991; Sawczyn et al., 2012; Brinzer et al., 2015). Additional metabolites like xylitol and psicose indicated osmoprotective adjustments and alterations in hexose/pentose pathways (Hendrix and Salvucci, 1998; Brinzer et al., 2015). Altered levels of kynurenine and dopa pointed to tryptophan/tyrosine metabolism disruptions linked to oxidative stress (Arévalo-Cortes et al., 2022). Shifts in inositol, threitol, gluconic acid, and glucono-1,5-lactone suggested polyol pathway reprogramming and oxidative glucose metabolism (Yancey, 2005; Walters et al., 2009; Sano et al., 2022). In contrast, pirimiphos-methyl caused broad metabolic suppression. Xylose and cysteine were central metabolites, implicating pentose and sulfur metabolism relevant to antioxidant defense (Sharma et al., 1972; Barbehenn et al., 2013; Silva et al., 2021). Additional markers included aminoadipic acid (lysine degradation), methylhexose (glycolysis), and putrescine (polyamine stress response) (Sakamoto et al., 2021; Boukouvala et al., 2023; Kavallieratos et al., 2023).

In *T. molitor* larvae, EO exposure altered neurotransmitter and energy metabolism. Beta-alanine, norepinephrine, and isocitric acid emerged as key hubs, indicating TCA cycle disruption and oxidative stress (Adamo, 2008; Li et al., 2010; Borycz et al., 2012). Dopamine and uric acid also reflected redox imbalance (Hanna et al., 2015; Tasaki et al., 2017). Pirimiphos-methyl affected different targets. Hydroxynicotinic acid (nicotinate metabolism), xanthurernate (tryptophan degradation), and o-phosphoethanolamine (phospholipid metabolism) were central nodes (Kalita et al., 2016; Dai et al., 2021; Stejskal et al., 2021). These disruptions likely reflect oxidative stress and acetylcholinesterase inhibition.

In *A. diaperinus* adults, EO treatment altered sugar alcohol and amino acid metabolism, with xylitol, psicose, and arabinose highlighting shifts in osmotic regulation and energy homeostasis (Dawkar et al., 2013; Haji et al., 2015; Subekti et al., 2024). Hydroxyproline and histamine indicated structural recovery and immunomodulation (Andrić et al., 2014; Kavallieratos et al., 2019). Pirimiphos-methyl caused more systemic disruptions: methylgalactose and histamine were key hubs; elevated leucine and aminoethanol reflected protein turnover and membrane remodeling; xylonic acid indicated sugar oxidation (Teets et al., 2012; Dawkar et al., 2013; Sharma and Batra, 2016).

In *T. molitor* adults, EO altered amino acid and oxidative defense pathways. Citrulline, methionine sulfoxide, methylgalactose, and beta-alanine were highly connected, suggesting nitrogen detoxification and redox adaptation (Sterkel and Oliveira, 2017; Meyer et al., 2020). Pirimiphos-methyl exposure led to elevated lactic acid, fructose, and aminoadipic acid—markers of glycolytic shift, oxidative stress, and membrane stress (Golić et al., 2017; Boukouvala and Kavallieratos, 2020; Syme et al., 2022).

5. Conclusions

This study offers compelling evidence for the insecticidal potential of *C. myrrha* EO, emphasizing its relevance as a promising component in integrated pest management strategies for stored-product protection. The findings align with prior research on the bioactivity of *C. myrrha* and its compounds, such as furanoeudesma-1,3-diene, lindestrene, isofuranodiene and curzerene, reinforcing their viability for pest control applications. Notably, the metabolomic data provide strong support for the mortality results, revealing that the EO not only induces death in target species but also triggers significant physiological disruptions. These metabolic perturbations appear to correspond with species- and stage-specific susceptibilities. For instance, the EO exerts a more intense effect on *T. molitor* larvae, evidenced by their higher mortality rates and deeper metabolic shifts, whereas *A. diaperinus* displays consistent susceptibility across life stages, with a uniformly disrupted metabolic profile. This suggests that EO-based strategies could be customized to exploit the unique vulnerabilities of different pest stages, enhancing their effectiveness in pest management scenarios.

CRediT authorship contribution statement

Nickolas G. Kavallieratos: Writing – review & editing, Writing – original draft, Visualization, Validation, Supervision, Software, Resources, Project administration, Methodology, Investigation, Funding acquisition, Formal analysis, Conceptualization. **Maria C. Boukouvala:** Writing – review & editing, Writing – original draft, Visualization, Validation, Software, Methodology, Investigation, Formal analysis, Data curation, Conceptualization. **Demeter Lorentha S. Gidari:** Writing – review & editing, Writing – original draft, Visualization, Validation, Software, Methodology, Investigation, Formal analysis, Data curation, Conceptualization. **Constantin S. Filintas:** Writing – review & editing, Writing – original draft, Visualization, Validation, Software, Methodology, Investigation, Formal analysis, Data curation, Conceptualization. **Anna Skourti:** Writing – review & editing, Writing – original draft, Visualization, Validation, Software, Methodology, Investigation, Formal

analysis, Data curation, Conceptualization. **Filippo Maggi:** Writing – review & editing, Writing – original draft, Visualization, Validation, Supervision, Software, Resources, Methodology, Investigation, Funding acquisition, Formal analysis, Conceptualization. **Marta Ferrati:** Writing – review & editing, Writing – original draft, Visualization, Validation, Software, Methodology, Investigation, Formal analysis, Data curation, Conceptualization. **Riccardo Petrelli:** Writing – review & editing, Writing – original draft, Visualization, Validation, Software, Methodology, Investigation, Funding acquisition, Formal analysis, Conceptualization. **Eleonora Spinozzi:** Writing – review & editing, Writing – original draft, Visualization, Validation, Software, Methodology, Investigation, Formal analysis, Data curation, Conceptualization. **Cristina Teruzzi:** Writing – review & editing, Writing – original draft, Visualization, Validation, Software, Methodology, Investigation, Formal analysis, Data curation, Conceptualization. **Fabrizio Araniti:** Writing – review & editing, Writing – original draft, Visualization, Validation, Supervision, Software, Resources, Methodology, Investigation, Funding acquisition, Formal analysis, Data curation, Conceptualization.

Declaration of competing interest

The authors declare that they have no known competing financial interests or personal relationships that could have appeared to influence the work reported in this paper.

Acknowledgments

This work was in part supported by the Special Account of Research, Agricultural University of Athens (80375).

Appendix A. Supplementary data

Supplementary data to this article can be found online at https://doi.org/10.1016/j.jspr.2025.102772.

Data availability

Data will be made available on request.

References

Adamo, S.A., 2008. Norepinephrine and octopamine: linking stress and immune function across phyla. Invertebr. Surviv. J. 5, 12–19.
Adams, R.P., 2007. Identification of Essential Oil Components by Gas Chromatograhpy/Mass Spectrometry. Allured Publishing, Carol Stream, IL.
Alanazi, N.A.H., Alamri, A.A., Mashlawi, A.M., Almuzaini, N., Mohamed, G., Salama, S. A., 2024. Gas chromatography–mass spectrometry chemical profiling of *Commiphora myrrha* resin extracts and evaluation of larvicidal, antioxidant, and cytotoxic activities. Molecules 29, 1778.
Al-Fuhaid, N., 2017. Repellency and fumigant toxicity of *Aloe vera, Astragalus sarcocolla, Commiphora myrrha* and *Ferula assafoetida* L gum resin powders and methanol extracts against *Trogoderma granarium* everts. Int. J. Agric. Sci. 7, 597–604.
Andrić, G., Kljajić, P., Pražić-Golić, M., 2014. Residual efficacy of cypermethrin and pirimiphos-methyl against *Sitophilus granarius* (L.) and *Plodia interpunctella* (Hübner) on concrete surface. Pestic. Fitomed. 29, 275–281.
Arévalo-Cortes, A., Damania, A., Granada, Y., Zuluaga, S., Mejía, R., Triana-Chávez, O., 2022. Association of midgut bacteria and their metabolic pathways with zika infection and insecticide resistance in colombian *Aedes aegypti* populations. Viruses 14, 2197.
Athanassiou, C.G., Kavallieratos, N.G., Boukouvala, M.C., Mavroforos, M.E., Kontodimas, D.C., 2015. Efficacy of alpha-cypermethrin and thiamethoxam against *Trogoderma granarium* Everts (Coleoptera: Dermestidae) and *Tenebrio molitor* L. (Coleoptera: Tenebrionidae) on concrete. J. Stored Prod. Res. 62, 101–107.
Baldovini, N., Tomi, F., Casanova, J., 2001. Identification and quantitative determination of furanodiene, a heat-sensitive compound, in essential oil by ^{13}C-NMR. Phytochem. Anal. 12, 58–63.
Barbehenn, R.V., Kochmanski, J., Menachem, B., Poirier, L.M., 2013. Allocation of cysteine for glutathione production in caterpillars with different antioxidant defense strategies: a comparison of *Lymantria dispar* and *Malacosoma disstria*. Arch. Insect Biochem. Physiol. 84, 90–103.
Basu, S., Duren, W., Evans, C.R., Burant, C.F., Michailidis, G., Karnovsky, A., 2017. Sparse network modeling and metscape-based visualization methods for the analysis of large-scale metabolomics data. Bioinformatics 33, 1545–1553.
Benelli, G., Pavela, R., Iannarelli, R., Petrelli, R., Cappellacci, L., Cianfaglione, K., Afshar, F.H., Nicoletti, M., Canale, A., Maggi, F., 2017. Synergized mixtures of Apiaceae essential oils and related plant-borne compounds: larvicidal effectiveness on the filariasis vector *Culex quinquefasciatus* Say. Ind. Crops Prod. 96, 186–195.
Bertola, M., Mutinelli, F.A., 2021. A systematic review on viruses in mass-reared edible insect species. Viruses 13, 2280.
Borycz, J., Borycz, J.A., Edwards, T.N., Boulianne, G.L., Meinertzhagen, I.A., 2012. The metabolism of histamine in the *Drosophila* optic lobe involves an ommatidial pathway: β-alanine recycles through the retina. J. Exp. Biol. 215, 1399–1411.
Boukouvala, M.C., Kavallieratos, N.G., 2020. Effect of six insecticides on egg hatching and larval mortality of *Trogoderma granarium* Everts (Coleoptera: Dermestidae). Insects 11, 263.
Boukouvala, M.C., Romano, D., Kavallieratos, N.G., Stefanini, C., Canale, A., Benelli, G., 2021. Behavioral asymmetries affecting male mating success in *Tenebrio molitor* (Coleoptera: Tenebrionidae), an important edible species. J. Econ. Entomol. 114, 454–461.
Boukouvala, M.C., Kavallieratos, N.G., Žikić, V., Stanković, S., Milošević, M., Skourti, A., Lazarević, M., 2023. Sub-lethal effects of pirimiphos-methyl are expressed to different levels in wings of three stored-product coleopterans: a geometric morphometrics investigation. Insects 14, 430.
Brinzer, R.A., Henderson, L., Marchiondo, A.A., Woods, D.J., Davies, S.A., Dow, J.A., 2015. Metabolomic profiling of permethrin-treated *Drosophila melanogaster* identifies a role for tryptophan catabolism in insecticide survival. Insect Biochem. Mol. Biol. 67, 74–86.
Cotton, G., Anstee, J.H., 1991. A biochemical and structural study on the effects of methoprene on fat body development in *Locusta migratoria* L. J. Insect Physiol. 37, 525–539.
Dai, W.T., Li, J., Ban, L.P., 2021. Genome-wide selective signature analysis revealed insecticide resistance mechanisms in *Cydia pomonella*. Insects 13, 2.
Dawkar, V.V., Chikate, Y.R., Lomate, P.R., Dholakia, B.B., Gupta, V.S., Giri, A.P., 2013. Molecular insights into resistance mechanisms of lepidopteran insect pests against toxicants. J. Proteome Res. 12, 4727–4737.
Dekebo, A., Dagne, E., Sterner, O., 2002. Furanosesquiterpenes from *Commiphora sphaerocarpa* and related adulterants of true myrrh. Fitoterapia 73, 48–55.
Eidson, C.S., Schmittle, S.C., Goode, R.B., Lal, J.B., 1966. Induction of leukosis tumors with the beetle *Alphitobius diaperinus*. Am. J. Vet. Res. 27, 1053–1057.
Engell Dahl, J., Renault, D., 2022. Ecophysiological responses of the lesser mealworm *Alphitobius diaperinus* exposed to desiccating conditions. Front. Physiol. 13, 826458.
Feng, J., Xu, B., Ma, D., Hao, Z., Jia, Y., Wang, C., Wang, L., 2022. Metabolite identification in fresh wheat grains of different colors and the influence of heat processing on metabolites via targeted and non-targeted metabolomics. Food Res. Int. 160, 111728.
Ferri, I., Spano, M., Dell'Anno, M., Mannina, L., Rossi, L., 2024. Metabolomic profiling of *Tenebrio molitor* reared on chestnut shell-enriched substrate using NMR spectroscopy. Foods 13, 3757.
Gadir, S.A., Ahmed, I.M., 2014. *Commiphora myrrha* and *Commiphora africana* essential oils. J. Chem. Pharmaceut. Res. 6, 151–156.
Golić, M., Kljajić, P., Andrić, G., 2017. Residual efficacy of cypermethrin and pirimiphos-methyl against *Sitotroga cerealella* (Olivier) in wheat grain. Pestic. Fitomed. 32, 217–222.
Goodwin, M.A., Waltman, W.D., 1996. Transmission of *Eimeria*, viruses, and bacteria to chicks: darkling beetles (*Alphitobius diaperinus*) as vectors of pathogens. J. Appl. Poultry Res. 5, 51–55.
Gostel, M.R., Phillipson, P.B., Weeks, A., 2016. Phylogenetic reconstruction of the myrrh genus, *Commiphora* (Burseraceae), reveals multiple radiations in Madagascar and clarifies infrageneric relationships. Syst. Bot. 41, 67–81.
Gouesbet, G., Renault, D., Derocles, S.A., Colinet, H., 2025. Strong resistance to β-cyfluthrin in a strain of the beetle *Alphitobius diaperinus*: a de novo transcriptome analysis. Insect Sci. 32, 209–226.
Hagstrum, D.W., Klejdysz, T., Subramanyam, B., Nawrot, J., 2013. Atlas of Stored-Product Insects and Mites. AACC International, St. Paul, MN.
Haji, K.A., Thawer, N.G., Khatib, B.O., Mcha, J.H., Rashid, A., Ali, A.S., Jones, C., Bagi, J., Magesa, S.M., Ramsan, M.M., Garimo, I., Greer, G., Reithinger, R., Ngondi, J.M., 2015. Efficacy, persistence and vector susceptibility to pirimiphos-methyl (Actellic 300CS) insecticide for indoor residual spraying in Zanzibar. Parasites Vectors 8, 1–7.
Hanna, M.E., Bednářová, A., Rakshit, K., Chaudhuri, A., O'Donnell, J.M., Krishnan, N., 2015. Perturbations in dopamine synthesis lead to discrete physiological effects and impact oxidative stress response in *Drosophila*. J. Insect Physiol. 73, 11–19.
Hassan, B.A., Glover, E.K., Luukkanen, O., Kanninen, M., Jamnadass, R., 2019. *Boswellia* and *Commiphora* species as a resource base for rural livelihood security in the horn of Africa: a systematic review. Forests 10, 551.
Hendrix, D.L., Salvucci, M.E., 1998. Polyol metabolism in homopterans at high temperatures: accumulation of mannitol in aphids (Aphididae: Homoptera) and sorbitol in whiteflies (Aleyrodidae: Homoptera). Comp. Biochem. Physiol. Mol. Integr. Physiol. 120, 487–494.
Kalita, M.K., Haloi, K., Devi, D., 2016. Larval exposure to chlorpyrifos affects nutritional physiology and induces genotoxicity in silkworm *Philosamia ricini* (Lepidoptera: Saturniidae). Front. Physiol. 7, 535.
Kavallieratos, N.G., Michail, E.J., Boukouvala, M.C., Nika, E.P., Skourti, A., 2019. Efficacy of pirimiphos-methyl, deltamethrin, spinosad and silicoSec against adults and larvae of *Tenebrio molitor* L. on wheat, barley and maize. J. Stored Prod. Res. 83, 161–167.
Kavallieratos, N.G., Papanikolaou, N.E., Kazani, A.N., Boukouvala, M.C., Malesios, C., 2021. Using multilevel models to explore the impact of abiotic and biotic conditions

on the efficacy of pirimiphos-methyl against *Tenebrio molitor* L. Environ. Sci. Pollut. Res. 28, 17200–17207.
Kavallieratos, N.G., Bonacucina, G., Nika, E.P., Skourti, A., Georgakopoulou, S.K.C., Filintas, C.S., Panariti, A.M.E., Maggi, F., Petrelli, R., Ferrati, M., Spinozzi, E., Perinelli, D.G., Canale, A., Benelli, G., 2023. The type of grain counts: effectiveness of three essential oil-based nanoemulsions against *Sitophilus oryzae*. Plants 12, 813.
Kavallieratos, N.G., Eleftheriadou, N., Boukouvala, M.C., Skourti, A., Filintas, C.S., Gidari, D.L.S., Maggi, F., Rossi, P., Drenaggi, E., Morshedloo, M.R., Ferrati, M., Spinozzi, E., 2024a. Exploring the efficacy of four Apiaceae essential oils against nine stored-product pests in wheat protection. Plants 13, 533.
Kavallieratos, N.G., Boukouvala, M.C., Skourti, A., Filintas, C.S., Eleftheriadou, N., Gidari, D.L.S., Spinozzi, E., Ferrati, M., Petrelli, R., Cianfaglione, K., Maggi, F., 2024b. Essential oils from three Cupressaceae species as stored wheat protectants: will they kill different developmental stages of nine noxious arthropods? J. Stored Prod. Res. 105, 102232.
Kavallieratos, N.G., Eleftheriadou, N., Filintas, C.S., Boukouvala, M.C., Gidari, D.L.S., Skourti, A., Ntinokas, D., Ferrati, M., Spinozzi, E., Petrelli, R., Maggi, F., 2025. The potency of essential oils in combating stored-product pests: from nature to nemesis. Plants 14, 192.
Latha, S., Selvamani, P., Prabha, T., 2021. Pharmacological uses of the plants belonging to the genus *Commiphora*. Cardiovasc. Hematol. Agents Med. Chem. 19, 101–117.
Leung, A.Y., Foster, S., 1996. Encyclopedia of Common Natural Ingredients Used in Foods, Drugs and Cosmetics. J. Wiley & Sons, New York, NY.
Li, H.M., Sun, L., Mittapalli, O., Muir, W.M., Xie, J., Wu, J., Schemerhorn, B.J., Jannasch, A., Chen, J.Y., Zhang, F., Adamec, J., Murdock, L.L., Pittendrigh, B.R., 2010. Bowman-Birk inhibitor affects pathways associated with energy metabolism in *Drosophila melanogaster*. Insect Mol. Biol. 19, 303–313.
Lubbe, A., Verpoorte, R., 2011. Cultivation of medicinal and aromatic plants for specialty industrial materials. Ind. Crops Prod. 34, 785–801.
Maggi, F., Barboni, L., Papa, F., Caprioli, G., Ricciutelli, M., Sagratini, G., Vittori, S., 2012. A forgotten vegetable (*Smyrnium olusatrum* L., Apiaceae) as a rich source of isofuranodiene. Food Chem. 135, 2852–2862.
Mansingh, A., 1965. The effect of malathion on the metabolism of amino acids in the German cockroach *Blattella germanica*. J. Insect Physiol. 11, 1389–1400.
Marongiu, B., Piras, A., Porcedda, S., Scorciapino, A., 2005. Chemical composition of the essential oil and supercritical CO_2 extract of *Commiphora myrrha* (Nees) Engl. and of *Acorus calamus* L. J. Agric. Food Chem. 53, 7939–7943.
Martínez, L.C., Plata-Rueda, A., Colares, H.C., Campos, J.M., Dos, Santos, Fernandes, F. L., Serrao, J.E., Zanuncio, J.C., 2018. Toxic effects of two essential oils and their constituents on the mealworm beetle, *Tenebrio molitor*. Bull. Entomol. Res. 108, 716–725.
Mekonnen, Z., Worku, A., Yohannes, T., Bahru, T., Mebratu, T., Teketay, D., 2013. Economic contribution of gum and resin resources to household livelihoods in selected regions and the national economy of Ethiopia. Ethnobot. Res. Appl. 11, 273–288.
Mewis, I., Ulrichs, C., 2001. Action of amorphous diatomaceous earth against different stages of the stored product pests *Tribolium confusum, Tenebrio molitor, Sitophilus granarius* and *Plodia interpunctella*. J. Stored Prod. Res. 37, 153–164.
Meyer, S., Gessner, D.K., Braune, M.S., Friedhoff, T., Most, E., Höring, M., Liebisch, G., Zorn, H., Eder, K., Ringseis, R., 2020. Comprehensive evaluation of the metabolic effects of insect meal from *Tenebrio molitor* L. in growing pigs by transcriptomics, metabolomics and lipidomics. J. Anim. Sci. Biotechnol. 11, 1–19.
Misra, B., 2019. Steps for building an open source EI-MS mass spectral library for GC-MS -based metabolomics. https://www.protocols.io/view/steps-for-building-an-opensource-ei-ms-mass-spect-8txhwpn.html.
Mondello, L., 2015. Mass Spectra of Flavors and Fragrances of Natural and Synthetic Compounds. Wiley, New York, NY.
Morteza-Semnani, K., Saeedi, M., 2003. Constituents of the essential oil of *Commiphora myrrha* (Nees) Engl. var. *molmol*. J. Essent. Oil Res. 15, 50–51.
Mukerjea, T.D., 1953. The relationship between the stage of development and susceptibility to DDT and the pyrethrins of *Diataraxia oleracea* (L.), *Tenebrio molitor* L., and *Periplaneta americana* (L.). Bull. Entomol. Res. 44, 121–161.
NIST23 (National Institute of Standards and Technology), 2023. NIST/EPA/NIH Mass Spectral Database. United States Department of Commerce, Gaithersburg, MD. https://www.nist.gov/srd/nist-standard-reference-database-1a.
Ntalli, N., Skourti, A., Nika, E.P., Boukouvala, M.C., Kavallieratos, N.G., 2021. Five natural compounds of botanical origin as wheat protectants against adults and larvae of *Tenebrio molitor* L. and *Trogoderma granarium* Everts. Environ. Sci. Pollut. Res. 28, 42763–42775.
Pavela, R., Pavoni, L., Bonacucina, G., Cespi, M., Kavallieratos, N.G., Cappellacci, L., Petrelli, R., Maggi, F., Benelli, G., 2019. Rationale for developing novel mosquito larvicides based on isofuranodiene microemulsions. J. Pest Sci. 92, 909–921.
Pedersen, K.E., Pedersen, N.N., Meyling, N.V., Fredensborg, B.L., Cedergreen, N., 2020. Differences in life stage sensitivity of the beetle *Tenebrio molitor* towards a pyrethroid insecticide explained by stage-specific variations in uptake, elimination and activity of detoxifying enzymes. Pestic. Biochem. Physiol. 162, 113–121.
Perumalsamy, H., Kim, N.J., Ahn, Y.J., 2009. Larvicidal activity of compounds isolated from *Asarum heterotropoides* against *Culex pipiens* pallens, *Aedes aegypti*, and *Ochlerotatus togoi* (Diptera: Culicidae). J. Med. Entomol. 46, 1420–1423.
Rees, D.P., 2004. Insects of Stored Products. CSIRO Publishing, Collingwood, Australia.
Renault, D., Colinet, H., 2021. Differences in the susceptibility to commercial insecticides among populations of the lesser mealworm *Alphitobius diaperinus* collected from poultry houses in France. Insects 12, 309.
Sakamoto, T., Sasaki, S., Yamaguchi, N., Nakano, M., Sato, H., Iwabuchi, K., Tabunoki, H., Simpson, R.J., Bono, H., 2021. De novo transcriptome analysis for examination of the nutrition metabolic system related to the evolutionary process through which stick insects gain the ability of flight (Phasmatodea). BMC Res. Notes 14, 182.
Sall, J., Lehman, A., Creighton, L., 2001. JMP Start Statistics. A Guide to Statistics and Data Analysis Using JMP and JMP IN Software. Duxbury Press, Belmont, CA.
Sammarco, B.C., Hinkle, N.C., Crossley, M.S., 2023. Biology and management of lesser mealworm *Alphitobius diaperinus* (Coleoptera: Tenebrionidae) in broiler houses. J. Integr. Pest Manag. 14, 2.
Sano, H., Nakamura, A., Yamane, M., Niwa, H., Nishimura, T., Araki, K., Takemoto, K., Ishiguro, K., Aoki, H., Kato, Y., Kojima, M., 2022. The polyol pathway is an evolutionarily conserved system for sensing glucose uptake. PLoS Biol. 20, e3001678.
SAS Institute Inc, 2021. Using JMP 16.2. SAS Institute Inc., Cary, NC.
Sawczyn, T., Dolezych, B., Klosok, M., Augustyniak, M., Stygar, D., Buldak, R.J., Kukla, M., Michalczyk, K., Karcz-Socha, I., Zwirska-Korczala, K., 2012. Alteration of carbohydrates metabolism and midgut glucose absorption in *Gromphadorhina portentosa* after subchronic exposure to imidacloprid and fenitrothion. J. Environ. Sci. Health A 47, 1644–1651.
Scheff, D.S., Arthur, F.H., 2018. Fecundity of *Tribolium castaneum* and *Tribolium confusum* adults after exposure to deltamethrin packaging. J. Pest Sci. 91, 717–725.
Sharma, G.K., Rock, G.C., Hodgson, E., 1972. Metabolism of sulphur amino acids via the cystathionine pathway in *Argyrotaenia velutinana* larvae. J. Insect Physiol. 18, 1333–1341.
Sharma, A., Batra, A., 2016. Primary metabolite profiling of *Tinospora cordifolia*. Nat. Prod. Chem. Res. 4, 1–7.
Shen, T., Li, G.H., Wang, X.N., Lou, H.X., 2012. The genus *Commiphora*: a review of its traditional uses, phytochemistry and pharmacology. J. Ethnopharmacol. 142, 319–330.
Silva, P.C., Ceja-Navarro, J.A., Azevedo, F., Karaoz, U., Brodie, E.L., Johansson, B., 2021. A novel d-xylose isomerase from the gut of the wood feeding beetle *Odontotaenius disjunctus* efficiently expressed in *Saccharomyces cerevisiae*. Sci. Rep. 11, 4766.
Singh, S., Kaur, M., Sharma, D.K., 2022. Broad-spectrum activity of essential oils in managing stored grain insect pests. Indian J. Entomol. 83, 854–864.
Snedecor, G.W., Cochran, W.G., 1989. Statistical Methods. Iowa State University Press, Iowa, IA.
Sokal, R.R., Rohlf, F.J., 1995. Biometry. Freeman & Company, New York, NY.
Soromessa, T., 2013. Ecological phytogeography: a case study of *Commiphora* species. Sci. Technol. Arts Res. J. 2, 93–104.
Spinozzi, E., Ferrati, M., Baldassarri, C., Rossi, P., Favia, G., Cameli, G., Benelli, G., Canale, A., De Fazi, L., Pavela, R., Quassinti, L., Giordani, C., Araniti, F., Cappellacci, L., Petrelli, R., Maggi, F., 2025. Essential oil and furanosesquiterpenes from myrrh oleo-gum resin: a breakthrough in mosquito vector management. Nat. Prod. Bioprospect 15, 12.
Stejskal, V., Stara, J., Pekar, S., Nesvorna, M., Hubert, J., 2021. Sensitivity of polyphagous (*Plodia interpunctella*) and stenophagous (*Ephestia kuehniella*) storage moths to residual insecticides: effect of formulation and larval age. Insect Sci. 28, 1734–1744.
Sterkel, M., Oliveira, P., 2017. Developmental roles of tyrosine metabolism enzymes in the blood-sucking insect *Rhodnius prolixus*. Proc. R. Soc. B. 284, 20162607.
Su, S., Wang, T., Duan, J.A., Zhou, W., Hua, Y.Q., Tang, Y.P., Yu, L., Qian, D.W., 2011. Anti-inflammatory and analgesic activity of different extracts of *Commiphora myrrha*. J. Ethnopharmacol. 134, 251–258.
Subekti, N., Salsabila, S., Fadhila, A., 2024. Efficacy test of insectiside with pirimiphos-methyl and alpha-cypermethrin on *Musa domestica* using surface spraying method. IOP Conf. Ser. Earth Environ. Sci. 1362, 012050.
Suleiman, M.H.A., 2015. Prenylated flavonoids from the stem wood of *Commiphora opobalsamum*. (L.) Engl. (Burseraceae). J. King Saud. Univ. Sci. 27, 71–75.
Sumner, L.W., Amberg, A., Barrett, D., Beale, M.H., Beger, R., Daykin, C.A., Fan, W.M.T., Fiehn, O., Goodacre, R., Griffin, J.L., Hankemeier, T., Hardy, N., Harnly, J., Higashi, R., Kopka, J., Lane, A.N., Lindon, J.C., Marriott, P., Nicholls, A.W., Reily, M. D., Thaden, J.J., Viant, M.R., 2007. Proposed minimum reporting standards for chemical analysis: chemical analysis working group (CAWG) metabolomics standards initiative (MSI). Metabolomics 3, 211–221.
Syme, T., Gbegbo, M., Obuobi, D., Fongnikin, A., Agbevo, A., Todjinou, D., Ngufor, C., 2022. Pyrethroid-piperonyl butoxide (PBO) nets reduce the efficacy of indoor residual spraying with pirimiphos-methyl against pyrethroid-resistant malaria vectors. Sci. Rep. 12, 6857.
Tasaki, E., Sakurai, H., Nitao, M., Matsuura, K., Iuchi, Y., 2017. Uric acid, an important antioxidant contributing to survival in termites. PLoS One 12, e0179426.
Teets, N.M., Peyton, J.T., Ragland, G.J., Colinet, H., Renault, D., Hahn, D.A., Denlinger, D.L., 2012. Combined transcriptomic and metabolomic approach uncovers molecular mechanisms of cold tolerance in a temperate flesh fly. Physiol. Genom. 44, 764–777.
Tipton, D.A., Lyle, B., Babich, H., Dabbous, M.K., 2003. In vitro cytotoxic and anti-inflammatory effects of myrrh oil on human gingival fibroblasts and epithelial cells. Toxicol. Vitro 17, 301–310.
Utpott, M., Rodrigues, E., de Oliveira Rios, A., Mercali, G.D., Flôres, S.H., 2022. Metabolomics: an analytical technique for food processing evaluation. Food Chem. 366, 130685.
Van den Dool, H., Krat, P.D., 1963. A generalization of the retention index system including linear temperature programmed gas-liquid partition chromatography. J Chromatogr. 2, 463–471.
Velusamy, R., Ponnudurai, G., Harikrishnan, T.J., 2020. Evaluation of the effect of essential oils (eucalyptus and lemon grass) against the darkling beetle. *Alphitobius diaperinus*. J. Entomol. Zool. Stud. 8, 1592–1595.

Walters, K.R., Pan, Q., Serianni, A.S., Duman, J.G., 2009. Cryoprotectant biosynthesis and the selective accumulation of threitol in the freeze-tolerant Alaskan beetle, *Upis ceramboides*. J. Biol. Chem. 284, 16822–16831.

Yancey, P.H., 2005. Organic osmolytes as compatible, metabolic and counteracting cytoprotectants in high osmolarity and other stresses. J. Exp. Biol. 208, 2819–2830.

Zar, J.H., 2014. Biostatistical Analysis. Pearson, Essex, UK.